

RESEARCH

Open Access



# Population-based analysis of ocular *Chlamydia trachomatis* in trachoma-endemic West African communities identifies genomic markers of disease severity

A. R. Last<sup>1\*</sup>, H. Pickering<sup>1</sup>, C. h. Roberts<sup>1</sup>, F. Coll<sup>2</sup>, J. Phelan<sup>2</sup>, S. E. Burr<sup>1,3</sup>, E. Cassama<sup>4</sup>, M. Nabicassa<sup>4</sup>, H. M. B. Seth-Smith<sup>5,6,7</sup>, J. Hadfield<sup>5</sup>, L. T. Cutcliffe<sup>8</sup>, I. N. Clarke<sup>8</sup>, D. C. W. Mabey<sup>1</sup>, R. L. Bailey<sup>1</sup>, T. G. Clark<sup>2,9</sup>, N. R. Thomson<sup>2,5</sup> and M. J. Holland<sup>1</sup>

## Abstract

**Background:** *Chlamydia trachomatis* (*Ct*) is the most common infectious cause of blindness and bacterial sexually transmitted infection worldwide. *Ct* strain-specific differences in clinical trachoma suggest that genetic polymorphisms in *Ct* may contribute to the observed variability in severity of clinical disease.

**Methods:** Using *Ct* whole genome sequences obtained directly from conjunctival swabs, we studied *Ct* genomic diversity and associations between *Ct* genetic polymorphisms with ocular localization and disease severity in a treatment-naïve trachoma-endemic population in Guinea-Bissau, West Africa.

**Results:** All *Ct* sequences fall within the T2 ocular clade phylogenetically. This is consistent with the presence of the characteristic deletion in *trpA* resulting in a truncated non-functional protein and the ocular tyrosine repeat regions present in *tarP* associated with ocular tissue localization. We have identified 21 *Ct* non-synonymous single nucleotide polymorphisms (SNPs) associated with ocular localization, including SNPs within *pmpD* (odds ratio, OR = 4.07,  $p^* = 0.001$ ) and *tarP* (OR = 0.34,  $p^* = 0.009$ ). Eight synonymous SNPs associated with disease severity were found in *yjfh* (*rlmB*) (OR = 0.13,  $p^* = 0.037$ ), *CTA0273* (OR = 0.12,  $p^* = 0.027$ ), *trmD* (OR = 0.12,  $p^* = 0.032$ ), *CTA0744* (OR = 0.12,  $p^* = 0.041$ ), *glgA* (OR = 0.10,  $p^* = 0.026$ ), *alaS* (OR = 0.10,  $p^* = 0.032$ ), *pmpE* (OR = 0.08,  $p^* = 0.001$ ) and the intergenic region *CTA0744–CTA0745* (OR = 0.13,  $p^* = 0.043$ ).

**Conclusions:** This study demonstrates the extent of genomic diversity within a naturally circulating population of ocular *Ct* and is the first to describe novel genomic associations with disease severity. These findings direct investigation of host-pathogen interactions that may be important in ocular *Ct* pathogenesis and disease transmission.

**Keywords:** *Chlamydia trachomatis*, Trachoma, Disease severity, Genome-wide association analysis, Single nucleotide polymorphisms, Pathogen genomic diversity

\* Correspondence: [anna.last@lshtm.ac.uk](mailto:anna.last@lshtm.ac.uk)

<sup>1</sup>Clinical Research Department, London School of Hygiene and Tropical Medicine, Keppel Street, London, UK

Full list of author information is available at the end of the article



## Background

The obligate intracellular bacterium *Chlamydia trachomatis* (*Ct*) is the leading infectious cause of blindness (trachoma) and the most common sexually transmitted bacterial infection [1, 2].

*Ct* strains are differentiated into biovars based on pathobiological characteristics and serovars based on serological reactivity for the major outer membrane protein (MOMP) encoded by *ompA* [3]. Serovars largely differentiate biological groups associated with trachoma (A–C), sexually transmitted disease (D–K) and lymphogranuloma venereum (LGV) (L1–L3). Despite diverse biological phenotypes, *Ct* strains share near complete genomic synteny and gene content [4], suggesting that minor genetic changes influence pathogen-host and tissue-specific infection characteristics [5–8]. All published African ocular *Ct* genomes are situated on the ocular branch within the T2 clade of non-LGV urogenital isolates [4]. Currently there are only 31 published ocular *Ct* genome sequences [4, 9–12].

The pathogenesis of chlamydial infection begins with epithelial inflammation and may progress to chronic immunofibrogenic processes leading to blindness and infertility, though many *Ct* infections do not result in sequelae [13, 14]. Strain-specific differences related to clinical presentation have been investigated in trachoma [8, 15, 16]. These studies examined a small number of ocular *Ct* isolates from the major trachoma serotypes and found a small subset of genes in addition to *ompA* that were associated with differences in in vitro growth rate, burst size, plaque morphology, interferon gamma (IFN $\gamma$ ) sensitivity and, most importantly, intensity of infection and clinical disease severity in non-human primates (NHPs), suggesting that genetic polymorphisms in *Ct* may contribute to the observed variability in severity of trachoma in endemic communities [8].

The obligate intracellular development of *Ct* has presented significant technical barriers to basic research into chlamydial biology. Only recently has genetic manipulation of the chlamydial plasmid been possible, allowing in vitro transformation and modification studies, though this remains technically challenging, necessitating alternative approaches [17, 18].

Whole genome sequencing (WGS) has recently been used to identify regions of likely recombination in recent clinical isolates, demonstrating that WGS analysis may be an effective approach for the discovery of loci associated with clinical presentation [6]. Additionally, a number of putative virulence factors have been identified through WGS analysis and subsequent in vitro and animal studies [5, 19–30]. However, there are currently no published population-based studies of *Ct* using WGS with corresponding detailed clinical data, making it difficult to relate genetic changes to functional relevance and virulence factors in vivo.

There is an increasing pool of *Ct* genomic data, largely from archived samples following cell culture and more recently directly from clinical samples [31]. WGS data obtained directly from clinical samples can be preferable to using WGS data obtained from cell-cultured *Ct*, since repeated passage of *Ct* results in mutations that are not observed in vivo [32–34].

*Ct* bacterial load is associated with disease severity, particularly conjunctival inflammation, in active (infective) trachoma [35]. Conjunctival inflammation has previously been shown to be a marker of severe disease and plays an important role in the pathogenesis of scarring trachoma [36–38]. In this study we used principal component analysis (PCA) to reduce the dimensions of clinical grade of inflammation (defined using the P score from the follicles, papillary hypertrophy, conjunctival scarring (FPC) trachoma grading system [39]) and *Ct* bacterial load to a single metric to define an in vivo conjunctival phenotype in active (infective) trachoma. PCA is a recognized dimension reduction technique used to combine multiple correlated traits into their uncorrelated principal components (PCs) [40–42], allowing us to examine the relationship between *Ct* genotype and disease severity. These data from the trachoma-endemic region of the Bijagós Archipelago of Guinea-Bissau currently represent the largest collection of ocular *Ct* sequences from a single population and provide a unique opportunity to gain insight into ocular *Ct* pathogenesis in humans.

## Methods

### Survey, clinical examination and sample collection

Survey, clinical examination and sample collection methods have been described previously [43, 44]. Briefly, we conducted a cross-sectional population-based survey in trachoma-endemic communities on the Bijagós Archipelago of Guinea-Bissau. The upper tarsal conjunctivae of each consenting participant were examined, digital photographs were taken, a clinical trachoma grade was assigned and two sequential conjunctival swabs were obtained from the left upper tarsal conjunctiva of each individual using a standardized method [43]. DNA was extracted and *Ct omcB* (genomic) copies/swab quantified from the second conjunctival swab using droplet digital polymerase chain reaction (ddPCR) [44, 45].

We used the modified FPC grading system for trachoma [39]. The modified FPC system allows detailed scoring of the conjunctiva for the presence of follicles (F score), papillary hypertrophy (conjunctival inflammation) (P score) and conjunctival scarring (C score), assigning a grade of 0–3 for each parameter. A single validated grader conducted the examinations, and these were verified by an expert grader (masked to the field grades and ddPCR results) using the digital photographs. Grader concordance was measured using Cohen's kappa, where a kappa > 0.9 was used as the threshold to indicate good agreement.

Conjunctival inflammation (P score) is known to have a strong association with *Ct* bacterial load in this and other populations [35, 46–49]. For this study we used PCA to combine the presence of inflammation (defined by the P score using the FPC trachoma grading system [39]) with *Ct* bacterial load (defined by tertile cut-offs illustrated in Additional file 1: Figure S1) [50]. The conjunctival disease phenotype is a dimension reduction of these two variables, defining what we observed in the conjunctiva at the time of sampling (Fig. 1). Dimension reduction using PCA to define complex disease phenotypes in genome-wide association studies (GWASs) is well recognized, as it allows multiple traits to be included to capture a more complex phenotype and accounts for correlation between traits. This approach therefore may reveal novel loci or pathways that would not be evident in a single-trait GWAS, where the full extent of genetic variation cannot be captured [40].

#### Preparation of chlamydial DNA from cell culture

For eight specimens, WGS data were obtained following *Ct* isolation in cell culture (from the first conjunctival swab) as a preliminary exploration of *Ct* genomic diversity in this population. Briefly, samples were isolated in McCoy cell cultures by removing 100  $\mu$ l eluate from the original swab with direct inoculation onto a glass coverslip within a bijoux containing Dulbecco's modified Eagle's medium

(DMEM). The inocula were centrifuged onto cell cultures at 1800 rpm for 30 min. Following centrifugation the cell culture supernatant was removed and cycloheximide-containing DMEM was added to infected cells which were then incubated at 37 °C in 5% CO<sub>2</sub> for 3 days. Viable *Ct* elementary bodies (EBs) were observed by phase contrast microscopy. Cells were harvested and further passaged every 3 days until all isolates reached a multiplicity of infection between 50 and 90% in 2xT25 flasks. Each isolate was prepared and the EBs purified as described previously [51]. DNA was extracted from the purified EBs using the Promega Wizard Genomic Purification kit according to the manufacturer's protocol [52].

#### Pre-sequencing target enrichment

For the remaining specimens ( $n = 118$ ), WGS data were obtained directly from clinical samples. DNA baits spanning the length of the *Ct* genome were compiled by SureDesign and synthesized by SureSelect<sup>XT</sup> (Agilent Technologies, UK). The total DNA extracted from clinical samples was quantified and carrier human genomic DNA added to obtain a total of 3  $\mu$ g input for library preparation. DNA was sheared using a Covaris E210 acoustic focusing unit [31]. End-repair, non-templated addition of 3'-A adapter ligation, hybridization, enrichment PCR and all post-reaction clean-up steps were performed according to the SureSelect<sup>XT</sup> Illumina Paired-End Sequencing Library

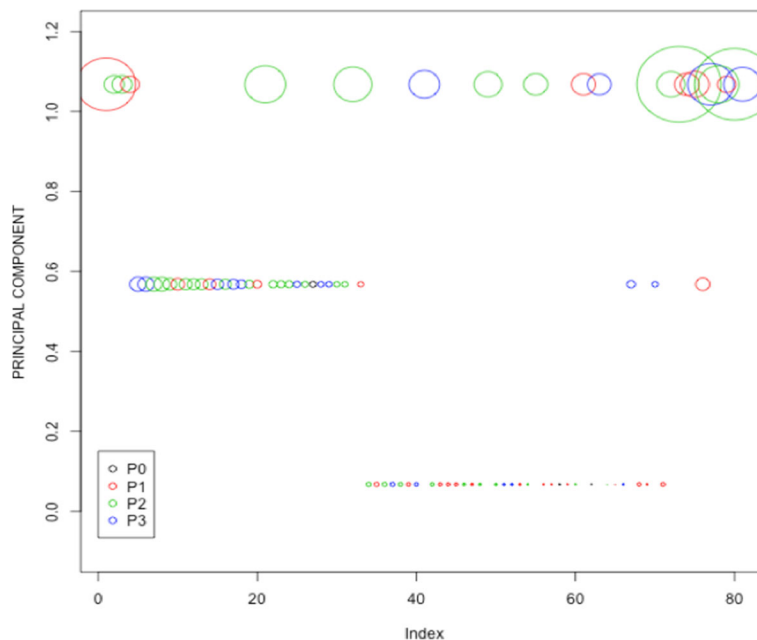


**Fig. 1** Composite in vivo conjunctival disease severity phenotype in ocular *Chlamydia trachomatis* infection. A composite in vivo phenotype was derived using principal component analysis (PCA) for dimension reduction of two phenotypic traits: a disease severity score (using the P score value) and *C. trachomatis* load (where *C. trachomatis* load was log transformed and cut-offs determined from the resulting density plot (see Additional file 1: Figure S1)). Each circle represents an individual infection (represented on the x-axis (Index),  $n = 81$ ). Circle size reflects *C. trachomatis* load and circle colour reflects inflammatory P score (P0–P3) defined using the modified FPC (follicles, papillary hypertrophy, conjunctival scarring) grading system for trachoma [39]

protocol (v1.4.1 Sept 2012). All recommended quality control measures were performed between steps.

**Whole genome sequencing and sequence quality filtering**

DNA was sequenced at the Wellcome Trust Sanger Institute using Illumina paired-end technology (Illumina GAI or HiSeq 2000). All 126 sequences passed standard FastQC quality control criteria [53]. Sequences were aligned to the most closely related reference genome, *Chlamydia trachomatis* A/HAR-13 (GenBank accession number NC\_007429.1 and plasmid GenBank accession number NC\_007430.1), using the Burrows-Wheeler Aligner (BWA) [54]. SAMtools/BCFtools (SAMtools v1.3.1) [55] and the Genome Analysis Tool Kit (GATK) [56] were used to call SNPs. We used standard GATK SNP calling algorithms, where > 10x depth of coverage is routinely used as the threshold value [56, 57]. This has been shown to be adequate for SNP calling in this context [57–59].

Variants were selected as the intersection data set between those obtained using both SNP callers and SNPs were further quality-filtered. SNP alleles were called using an alternative coverage-based approach where a missing call was assigned to a site if the total coverage was less than 20x depth or where one of the four nucleotides accounted for at least 80% total coverage [60]. There was a clear

relationship between the mean depth of coverage and the proportion of missing calls, based on which we retained sequences with greater than 10x mean depth of coverage over the whole genome (81 sequences retained).

Heterozygous calls were removed, and SNPs with a minor allele frequency (MAF) of less than 25% were removed. Samples with greater than 25% genome-wide missing data and 30% missing data per SNP were excluded from the analysis (n = 10, 71 sequences retained). All SNP positions with a MAF greater than 20% were identified using BCFtools v0.1.19 (<https://samtools.github.io/bcftools/>). Sequences were excluded from the final GWAS if more than 300 such positions were found using methods described by Hadfield et al. [61]. The quality assessment and filtering process is shown in Fig. 2. Details of the WGS data are provided in Additional file 2: Figure S2.

**Phylogenetic reconstruction**

Samples were mapped to the ocular reference strain *Ct* A/HAR-13 and SNPs were called as described above. Phylogenies were computed using RAxML v7.8.2 [62] from a variable sites alignment using a generalized time-reversible (GTR) + gamma model and are midpoint rooted. Recombination is known to occur in *Ct* [4, 6] and can be problematic in constructing phylogeny. We applied three

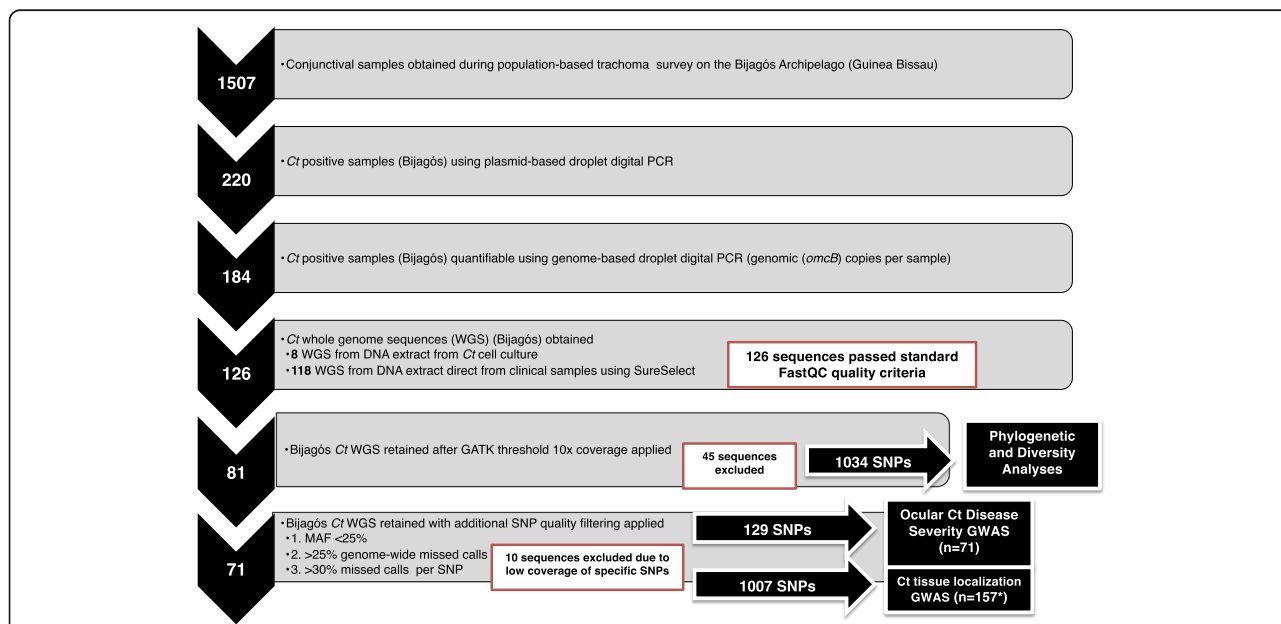


**Fig. 2** Whole genome sequencing (WGS) quality filtering processes and threshold criteria for inclusion in analyses. *Ct* DNA detected using droplet digital PCR [45]. WGS data were obtained using SureSelect target enrichment [31] (or chlamydial cell culture) and Illumina paired-end sequencing. FastQC [53] was used to assess basic WGS quality. SNP alleles were called against reference strain *Ct* A/HAR-13 using an alternative coverage-based approach where a missing call was assigned to a site if the total coverage was less than 20x depth or where one of the four nucleotides accounted for at least 80% total coverage [60]. There was a clear relationship between the mean depth of coverage and genome-wide proportion of missing calls; therefore, only sequences with greater than 10x mean depth of coverage over the whole genome were retained using the GATK Best Practices threshold [56, 57]. Heterozygous calls were removed and SNPs with a minor allele frequency (MAF) of less than 25% were removed. Samples with greater than 25% genome-wide missing data and 30% missing data per SNP were excluded from the analysis. WGS sequence quality is shown in detail in Additional file 12: Figure S12. \*n = 157 including the 71 Bijagós sequences in addition to 48 Rombo District sequences and 38 reference sequences

compatibility-based recombination detection methods to detect regions of recombination using PhiPack [63]: the pairwise homoplasmy index (Phi), the maximum  $\chi^2$  and the neighbour similarity score (NSS) across the genome alignment. We also examined the confidence in the phylogenetic tree by computing RAxML site-based likelihood scores [62]. Phylogenetic trees were examined adjusting for recombination using the methods described above.

Additionally, sequence data for the tryptophan operon (*CTA0182* and *CTA0184–CTA0186*), *tarP* (*CTA0498*), nine polymorphic membrane proteins (*CTA0447–CTA0449*, *CTA0884*, *CTA0949–CTA0952* and *CTA0954*) and *ompA* (*CTA0742*) were extracted from the 81 ocular *Ct* sequences from Guinea-Bissau retained after quality control filtering described above, 48 ocular sequences originating from a study conducted in Kahe village, Rombo District, Tanzania [64] and 38 publicly available reference sequences. Phylogenies were constructed as described above.

Polymorphisms, insertions and deletions (indels) and truncations for the tryptophan operon were manually determined from aligned sequences using SeaView [65]. Tyrosine repeat regions and actin-binding domains in *tarP* were found using RADAR [66] and Pfam [67] respectively.

#### Pairwise diversity

A comparison was made between the two population-based *Ct* sequence data sets from the Bijagós (Guinea-Bissau) and Rombo (Tanzania) sequences whereby short read data from the 81 Bijagós sequences and 48 Rombo sequences were mapped against *Ct A/HAR-13* using SAMtools. Within-population pairwise nucleotide diversity was calculated using the formula:

$$\pi = 2 \times \sum_{i=1}^n \sum_{j=1}^{i-1} x_i x_j \pi_{ij}$$

where  $n$  is the number of sequences,  $x$  is the frequency of sequences  $i$  and  $j$  and  $\pi_{ij}$  is the number of nucleotide differences per site between sequences  $i$  and  $j$  [68]. The frequency of sequences was considered uniform within the populations, and sites with missing calls were excluded on a per-sequence basis.

#### Genome-wide association analyses

To investigate the association between *Ct* polymorphisms with ocular localization and clinical disease severity, we used permutation-based logistic regression methods, which are powerful and well-recognized tools in GWAS, allowing for adjustment for population structure, age and gender in the model and accounting for multiple testing [69–72].

We used permutation analyses of 100,024 phenotypic resamplings, where the distribution of the  $p$  value was approximated by simulating data sets through randomization under the null hypothesis of no association between

phenotype and genotype. Genome-wide significance was determined as  $p^* \leq 0.05$ , where  $p^*$  was defined as the fraction of re-sampled (simulated) data that returned  $p$  values that were less than or equal to the  $p$  values observed in the data [50]. All analyses were conducted using the R statistical package v3.0.2 (the R Foundation for Statistical Computing, <https://www.r-project.org/>) using MASS, GLM and lsr. All R script used for these analyses is contained within Additional file 3: Figure S3 and is released as a CC-BY open resource (CC-BY-SA 3.0).

#### Ocular localization

Tissue localization is defined as the localization (or presence) of a detectable *Ct* infection to either the conjunctival epithelium or the urogenital tract. Short read data from the 129 clinical ocular sequences from the pairwise diversity analysis and 38 publicly available reference sequences from ocular ( $n = 8$ ), urogenital ( $n = 17$ ) and rectal ( $n = 13$ ) sites were mapped against *Ct A/HAR-13* using SAMtools. Only polymorphic sites were retained, and SNPs were filtered as described above. The final analysis includes 1007 SNPs from 157 sequences, a phylogeny of which is contained within Additional file 4: Figure S4. A permutation-based generalized linear regression model was used to test the association between collection site (ocular or urogenital tissue localization) and polymorphic sites. For each SNP the standard error for the  $t$  statistic was estimated from the model and used to calculate the odds ratios (ORs) and 95% confidence intervals. A  $\chi^2$  test was used to determine the association between ocular localization-associated SNPs and both gene expression stage and predicted localization of the encoded proteins. The developmental cycle expression stage for each transcript was based on data and groupings from Belland et al. [73]. Predicted localization of expressed proteins was defined using the consensus from three predictions using CELLO [74], PSORTb [75] and LocTree3 [76].

#### Clinical disease severity

A permutation-based ordinal logistic regression model was used to test the association between the disease severity score (using the in vivo conjunctival phenotype defined previously) and polymorphic sites. The final analysis includes 129 SNPs from 71 sequences derived as described in Fig. 2. For each SNP the standard error for the  $t$  statistic was estimated from the model and used to calculate the ORs and 95% confidence intervals. Individuals' age and gender were included as a covariate to the regression analysis.

We investigated the effect of population structure on the results of the GWAS analysis using PCA [77]. The first three PCs captured the majority of structural variation, but including them in the model had no effect; therefore, they were not included in the final model.

We corrected for genomic inflation if the occurrence of a polymorphism in the population was more than 90% or if there was a MAF of 3%.

## Results

Conjunctival swabs collected during a cross-sectional population-based trachoma survey on the Bijagós Archipelago yielded 220 ocular *Ct* infections detected by *Ct* plasmid-based ddPCR. Of the 220 *Ct* infections detected, 184 were quantifiable using *Ct* genome-based ddPCR.

We obtained WGS data from 126/220 samples using cell culture ( $n = 8$ ) or direct sequencing from swabs with Sure-Select<sup>XT</sup> target enrichment ( $n = 118$ ), representing the largest cross-sectional collection of ocular *Ct* WGS. Eighty-one of these sequences were subsequently included in the phylogenetic and diversity analyses and 71 were retained in the final genome-wide association (tissue localization (derived from the anatomical site of sample collection) and disease severity) analyses. The quality filtering process is illustrated in Fig. 2 and detailed in Methods.

A total of 1034 unique SNP sites were identified within the 126 Bijagós *Ct* genomes relative to the reference strain *Ct A/HAR-13*. Following application of further threshold criteria based on MAF and genome-wide missing data thresholds, we retained only high-quality genomic data in the final association analyses (129 SNPs from 71 sequences). There were no significant differences between the 71 retained and the 55 excluded sequences with respect to demographic characteristics, bacterial load, disease severity scores or geographical location (Table 1). Clinical and demographic details of the survey participants in whom we did not identify *Ct* infection have been published previously [43]. Of the ten SNPs initially identified within the *Ct* plasmid sequences, none fulfilled the quality filtering criteria, and they were not retained for the genome-wide association analyses.

### Ocular *C. trachomatis* phylogeny and diversity

For the phylogeny and diversity analyses, 81 Bijagós *Ct* sequences were included on the basis of the quality filtering criteria described in detail in Fig. 2. SNP-based phylogenetic trees constructed using all 1034 SNPs for sequences above 10× coverage ( $n = 81$ ), with 54 published *Ct* reference genomes, are shown in Fig. 3.

The Bijagós sequences are situated within the T2 ocular monophyletic lineage with all other ocular *Ct* sequences [59] except those described by Andersson et al. [10]. However, our population-based collection of ocular *Ct* sequences has much greater diversity at whole genome resolution than previously demonstrated in African trachoma isolates [4, 8]. We used a pairwise diversity ( $\pi$ ) metric to compare two populations of ocular *Ct* from regions with similar trachoma endemicity and studies with similar design, sample size and available epidemiological

metadata. These data show much greater genomic diversity in the Bijagós ocular *Ct* sequences ( $\pi = 0.07167$ ) compared to the Tanzanian (Rombo) ocular *Ct* sequences ( $\pi = 0.00047$ ).

By *ompA* genotyping, 73 of the Bijagós sequences are genotype A and 8 are genotype B, supporting their classical ocular nature (Additional file 5: Figure S5). The high resolution of WGS data obtained directly from clinical samples captures diversity that may be useful in strain classification, particularly as we found some evidence of clustering at village level, although the very small number of sequences per village means that it is not possible to provide accurate estimates of clustering in this study (Fig. 4).

Homoplastic SNPs and regions affected by recombination are shown in Additional file 6: Figure S6a. Removal of these regions of recombination identified using the pairwise homoplasy index had no effect on phylogenetic relationships. Additionally, a site-wise log likelihood plot demonstrated that there was no clear genomic region where there was significant lack of confidence in the tree construction due to recombination (Additional file 6: Figure S6b). Whether regions containing recombination were included or excluded, tree topology remained essentially identical, indicating that branching order is not affected by the removal of these regions.

### Genome-wide analysis of *C. trachomatis* localization

Candidate genes thought to be involved in or indicative of ocular localization or preference were examined to further characterize this population of ocular *Ct*. Polymorphisms and truncations in the tryptophan operon have previously been implicated in the inability of ocular *Ct* to infect and survive in the genital tract [5]. All sequences contained mutations in *trpA* resulting in truncation. The majority (80/81) were truncated at the previously characterized deletion at position 533 [5]. Polymorphisms in *trpB* and *trpR* were less common (Additional file 7: Figure S7).

The variable domain structure of the translocated actin-recruiting phosphoprotein (*tarP*) has also been implicated in tropism [78]. Ocular strains possess more actin-binding domains (three or four) and fewer tyrosine repeat regions (between one and three). Urogenital strain *tarP* sequences have low copy numbers of both, and LGV strain sequences have additional tyrosine repeat regions. In this study, all sequences contain the expected three tyrosine repeat regions and three or four actin-binding domains (Additional file 7: Figure S7).

The nine virulence-associated polymorphic membrane proteins (Pmp) are variably related to tissue preference, with all encoding genes except *pmpA*, *pmpD* and *pmpE* clustering by tissue location [20]. In this population all phylogenies of the six tropism-clustering *pmps* show that all sequences cluster with other ocular sequences (Additional file 8: Figure S8).

**Table 1** Characteristics of ocular *Chlamydia trachomatis* sequences included in the disease severity association analysis

Sequence ID	Sample ID	Average depth of coverage	% Missing reads <sup>a</sup>	Gender	Age (years)	Island code	Village code	Ocular load <sup>b</sup>	P score <sup>c</sup>
11152_3_1	14,344	764	0.35%	M	4	002	33	202,632	1
11152_3_10	17,347	121	0.21%	M	5	001	17	69,093	2
11152_3_11	4422	19	19.95%	F	2	001	12	68,782	2
11152_3_12	11,231	68	2.24%	M	0	003	43	64,036	1
11152_3_13	15,631	21	14.93%	F	2	002	33	55,749	3
11152_3_14	6105	1664	0.05%	F	1	001	14	55,202	3
11152_3_15	12,628	191	0.10%	F	12	002	29	54,651	2
11152_3_16	7524	2065	0.14%	M	10	002	35	54,539	2
11152_3_17	5016	61	0.44%	F	1	001	15	46,510	2
11152_3_18	1485	44	1.21%	F	4	002	27	45,929	1
11152_3_19	15,554	825	0.06%	F	1	002	33	44,052	2
11152_3_20	6094	3070	0.00%	F	3	001	14	42,917	2
11152_3_22	5082	51	0.81%	M	6	001	15	42,427	1
11152_3_23	12,969	3643	1.81%	F	3	002	29	41,308	3
11152_3_25	8140	246	0.36%	M	13	001	20	39,816	2
11152_3_26	6083	2746	0.00%	F	23	001	14	38,771	3
11152_3_27	16,621	1664	0.00%	M	3	002	37	33,514	3
11152_3_28	16,852	143	0.16%	M	5	002	38	31,228	2
11152_3_29	16,588	53	0.81%	M	6	002	37	29,991	1
11152_3_3	4180	51	0.92%	M	2	001	12	140,693	2
11152_3_30	7612	107	0.44%	F	3	002	35	28,528	2
11152_3_31	6985	177	0.10%	M	6	001	17	27,924	2
11152_3_32	4411	24	9.68%	F	1	001	12	27,584	2
11152_3_33	4257	381	0.06%	M	0	001	12	24,033	3
11152_3_34	4400	48	0.98%	M	6	001	12	23,435	2
11152_3_35	15,180	571	0.35%	F	7	002	33	23,254	0
11152_3_36	13,596	496	0.06%	M	18	002	23	22,098	3
11152_3_37	1672	20	18.42%	M	6	002	25	21,630	3
11152_3_38	5181	81	0.32%	M	4	001	15	21,339	2
11152_3_39	15,532	243	0.08%	F	25	002	33	21,174	2
11152_3_4	8074	150	0.13%	M	4	001	18	131,175	2
11152_3_40	16,984	145	0.19%	M	4	002	21	20,113	1
11152_3_41	1881	37	2.71%	F	1	002	32	15,963	2
11152_3_42	10,032	101	0.16%	M	2	003	42	15,706	1
11152_3_43	8492	70	2.60%	M	1	004	45	15,582	2
11152_3_44	13,585	31	4.97%	M	23	002	23	15,417	3
11152_3_48	7535	61	0.84%	M	18	002	35	13,439	3
11152_3_5	7095	235	0.44%	F	4	001	17	105,453	3
11152_3_50	6028	46	1.24%	F	4	001	14	12,961	2
11152_3_52	10,021	20	16.15%	F	6	003	42	11,840	1
11152_3_55	12,650	59	0.54%	M	6	002	29	9001	2
11152_3_57	8965	21	16.60%	M	27	003	43	7336	1
11152_3_58	5104	33	3.68%	M	2	001	15	7203	2

**Table 1** Characteristics of ocular *Chlamydia trachomatis* sequences included in the disease severity association analysis (Continued)

Sequence ID	Sample ID	Average depth of coverage	% Missing reads <sup>a</sup>	Gender	Age (years)	Island code	Village code	Ocular load <sup>b</sup>	P score <sup>c</sup>
11152_3_6	16,599	52	0.73%	M	9	002	37	96,333	2
11152_3_62	7062	22	13.41%	F	4	001	17	6986	3
11152_3_63	8778	17	25.47%	F	11	004	46	6760	3
11152_3_66	1892	45	1.25%	F	2	002	32	6374	1
11152_3_7	10,747	581	1.82%	F	3	003	44	82,916	2
11152_3_70	13,189	25	8.87%	F	3	002	24	4703	1
11152_3_74	15,499	24	10.49%	M	5	002	33	4226	1
11152_3_76	726	417	0.06%	F	3	002	26	3753	0
11152_3_77	7579	105	0.52%	F	5	002	35	3468	1
11152_3_78	12,089	16	27.78%	F	13	002	47	3203	2
11152_3_8	6996	38	2.03%	M	3	001	17	82,614	1
11152_3_88	748	163	0.10%	F	2	002	26	1636	0
11152_3_9	10,967	20	17.52%	F	2	003	44	81,124	3
11152_3_92	1463	73	0.30%	F	42	002	27	1273	2
13108_1_14	24,519	51	2.81%	M	2	004	45	29,040	3
13108_1_15	6941	33	1.81%	M	36	001	17	13,155	1
13108_1_7	25,124	27	5.27%	M	4	002	22	21,750	3
13108_1_9	22,154	18	20.56%	F	5	003	43	14,349	1
8422_8_49	2353	39	5.70%	M	11	002	35	96,889	2
8422_8_50	2366	82	1.08%	M	1	002	35	289,778	2
9471_4_86	12,980	287	1.90%	M	4	002	29	85,456	1
9471_4_87	15,367	215	0.46%	M	1	002	33	99,064	1
9471_4_88	15,543	192	0.11%	F	23	002	33	49,125	1
9471_4_89	1870	119	0.14%	M	3	002	32	158,548	3
9471_4_90	2145	111	0.11%	M	15	002	32	140,297	2
9471_4_91	4158	94	0.14%	M	4	001	12	63,654	1
9471_4_92	4169	85	0.13%	F	3	001	12	274,835	2
9471_4_93	7590	242	0.51%	F	1	002	35	128,025	3

Sequences ( $n = 55$ ) were excluded from the association analysis if there was (1)  $< 10\times$  coverage, (2)<sup>a</sup>  $> 25\%$  missing reads genome-wide and (3)  $> 25\%$  missing ( $N$ ) calls at the single nucleotide polymorphism (SNP) locus. Coverage and missing data were correlated and resulted in exclusion of the same samples irrespective of criteria chosen. Seventy-one sequences were retained in the final disease severity analysis. <sup>b</sup>Ocular *C. trachomatis* load = *omcB* (*C. trachomatis* genome) copies per conjunctival swab measured using droplet digital PCR. <sup>c</sup>P score = conjunctival inflammation score (0–3) using the modified FPC (follicles, papillary hypertrophy, conjunctival scarring) grading system for trachoma [39]

Permutation-based re-sampling methods, commonly used in GWAS analyses, were used to account for multiple comparisons [69–72]. We tested 1007 SNPs in 157 *Ct* sequences (Fig. 2) for association with ocular localization (defined by anatomical site of sample collection), comparing 127 ocular, 17 urogenital and 13 LGV strains (Fig. 5a). One hundred and five SNPs were significantly associated with ocular localization ( $p^* < 0.05$ ), of which 21 were non-synonymous (details in Table 2a and Additional file 9: Figure S9). These were within a number of genes known to be polymorphic, genes previously identified as tropism-associated (*CTA0156*, *CTA0498/tarP* and *CTA0743/pbpB*) and virulence factors (*CTA0498/tarP* and *CTA0884/pmpD*). Four genes contained multiple non-synonymous

SNPs (*CTA\_0733/karG*, *CTA\_089/5sucD*, *CTA\_0087* and *CTA\_0145/oppA\_1*), and ten genes contained multiple synonymous SNPs. Of the genes containing multiple synonymous SNPs, five contained more than three SNPs (*CTA\_0739/tsf*, *CTA\_0733/karG*, *CTA\_0156*, *CTA\_0154* and *CTA\_0153*). No predicted protein localization was over-represented in the ocular localization-related SNPs ( $p = 0.6174$ ); however, early and very-late expressed genes were over-represented ( $p = 0.0197$ ).

#### Markers of disease severity in ocular *C. trachomatis* infection

Using permutation-based re-sampling methods, eight SNPs were found to be significantly associated with



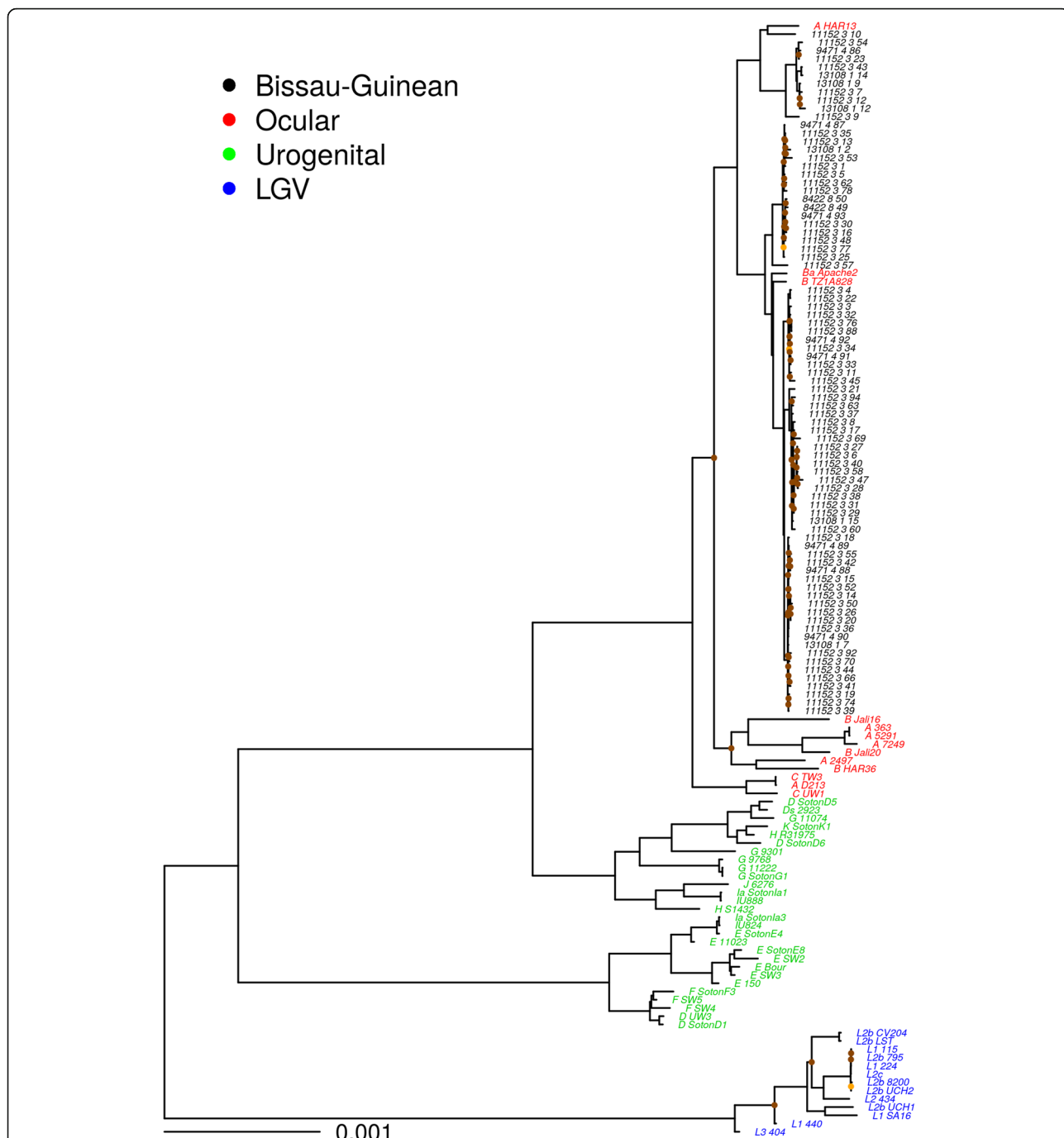
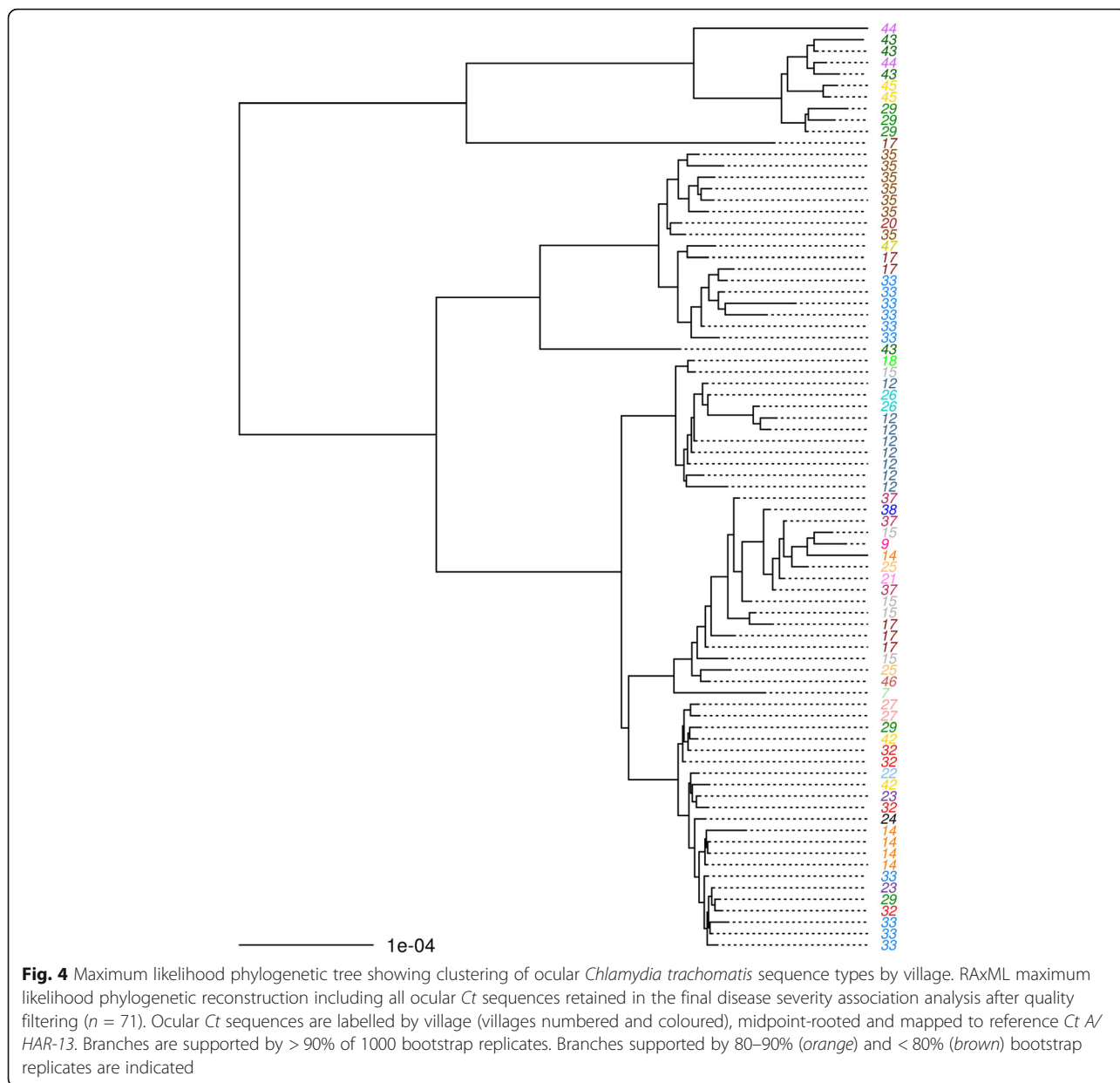


**Fig. 3** Maximum likelihood reconstruction of whole genome phylogeny of ocular *Chlamydia trachomatis* sequences from the Bijagós Archipelago (Guinea-Bissau). Maximum likelihood reconstruction of the whole genome phylogeny of 81 *Ct* sequences from the Bijagós Islands and 54 *Ct* reference strains. Bijagós *Ct* sequences ( $n = 81$ ) were mapped to *Ct A/HAR-13* using SAMtools [55]. SNPs were called as described by Harris et al. [4]. Phylogenies were computed with RAxML [62] from a variable sites alignment using a GTR + gamma model and are midpoint rooted. The scale bar indicates evolutionary distance. Bijagós *Ct* sequences in this study are coloured black, and reference strains are coloured by tissue localization (red = Ocular, green = Urogenital, blue = LGV). Branches are supported by > 90% of 1000 bootstrap replicates. Branches supported by 80–90% (orange) and < 80% (brown) bootstrap replicates are indicated

disease severity (Fig. 5b). Seven of these are in coding regions (relative to *Ct A/HAR-13*). Five are present at nucleotide positions 465,330 (OR = 0.13,  $p^* = 0.037$ ),

32,779 (OR = 0.12,  $p^* = 0.032$ ), 875,804 (OR = 0.10,  $p^* = 0.024$ ), 939,488 (OR = 0.10,  $p^* = 0.026$ ) and 1,028,728 (OR = 0.08,  $p^* = 0.013$ ) (where  $p^*$  is the permuted  $p$



value with a genome-wide threshold of 0.05) representing synonymous codon changes within the genes *yjfH*, *trmD*, *alaS*, *glgA* and *pmpE* respectively. Three further genome-wide significant synonymous SNPs were present at positions 827,184 (OR = 0.3,  $p^* = 0.041$ ) within the predicted coding sequence (CDS) *CTA0744*, 285,610 (OR = 0.12,  $p^* = 0.027$ ) within *CTA0273* and 787,841 (OR = 0.13,  $p^* = 0.043$ ) in the intergenic region between loci *CTA0744–CTA0745* (Table 2b and Additional file 10: Figure S10).

**Discussion**

This collection of clinical ocular *Ct* WGS from a single trachoma-endemic population to be characterized has

enabled us to describe the population diversity of naturally occurring *Ct* in a treatment-naïve population. We used detailed clinical grading combined with microbial quantitation to perform a GWAS and investigated associations between *Ct* polymorphisms with ocular localization and disease severity in trachoma.

Unlike the recently published Australian *Ct* sequences [10], all Bijagós sequences clustered as expected within the T2 ocular clade derived from a urogenital ancestor [59, 61], each with loci typically associated with ocular tissue localization (*trpA* and *tarP*). Although the Bijagós sequences conform to the classical ocular genotype, the phylogenetic data show greater than expected diversity compared to historical reference strains of ocular *Ct* [4] and a population of

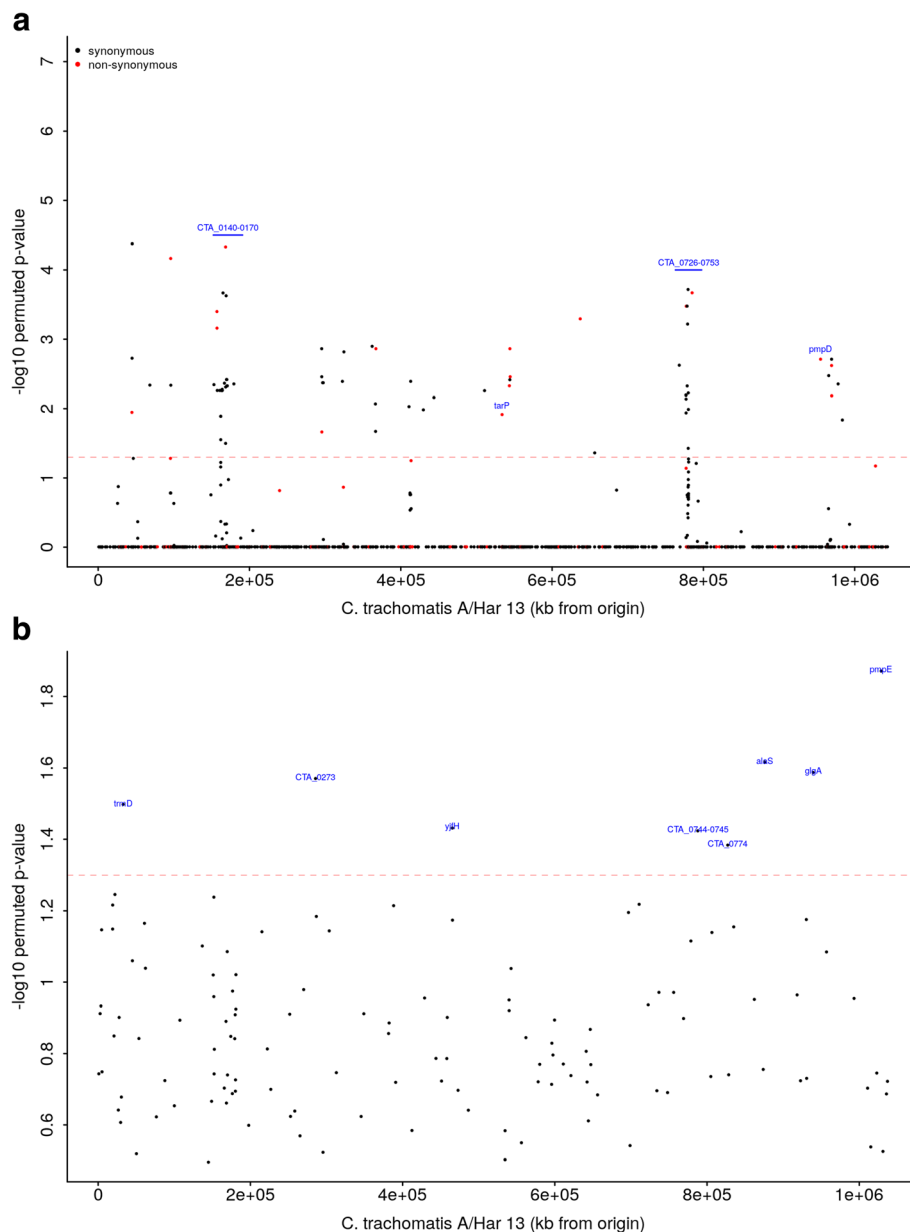


**Fig. 5** Single nucleotide polymorphisms on the *Chlamydia trachomatis* genome associated with **(a)** ocular localization and **(b)** disease severity at genome-wide significance. **a** Ocular localization-associated SNPs across the *C. trachomatis* genome. There were 1007 SNPs identified in coding and non-coding regions and included in permutation-based linear regression models in the *Ct* genome-wide association analysis. The threshold for genome-wide significance is indicated by the *dashed line* ( $p^* < 0.05$ ). The  $y$ -axis shows the  $-\log_{10} p$  value. A  $-\log_{10} p$  value of 1.3 is equivalent to a permuted  $p$  value of 0.05 ( $p^* < 0.05$ ). Synonymous (*black*) and non-synonymous SNPs (*red*) are indicated. Regions informative for ocular localization and genes of interest are labelled in *blue*. **b** Disease severity-associated SNPs across the *Ct* genome. From 129 SNPs identified in coding and non-coding regions, SNPs associated with the disease severity phenotype at genome-wide significance are identified using permutation-based ordinal logistic regression models adjusting for age in the *Ct* genome-wide association analysis. The threshold for genome-wide significance is indicated by the *dashed line* ( $p^* < 0.05$ ). The  $y$ -axis shows the  $-\log_{10} p$  value. A  $\log_{10} p$  value of 1.3 is equivalent to a permuted  $p$  value of 0.05 ( $p^* < 0.05$ ). Genes significantly associated with disease severity are labelled in *blue*

clinical ocular *Ct* sequences obtained from cultured clinical conjunctival swab specimens collected from another African trachoma-endemic population [64] (Additional file 4: Figure S4). Our use of direct WGS from clinical samples reveals the natural diversity of a population-based collection of

endemic treatment-naïve ocular *Ct* infections. This diversity may indicate genome-wide selection for advantageous mutations as demonstrated in other pathogens [79] or simply the naturally diverse circulation of endemic treatment-naïve ocular *Ct*.

**Table 2** SNPs across the *Chlamydia trachomatis* genome identified using permutation-based genome-wide association analysis for (A) ocular localization (non-synonymous only) and (B) disease severity

(A)															
SNP position	Ocular allele (%)	Urogenital allele (%)	Name A/HAR-13	CDS	p value	p*	OR	95% CI (UL)	95% CI (LL)	t	SE(t)	MAF	N calls at locus	Ocular AA	Urogenital AA
168413	A (61.54)	G (93.33)	CTA_0156	CDS	5E-05	1E-04	21.56	6.11	137.25	4.07	0.75	0.50	0.04	H	R
95863	A (60.47)	G (86.67)	CTA_0087	CDS	7E-05	1E-04	9.56	3.47	33.86	3.98	0.57	0.49	0.02	E	G
785083	A (62.20)	G (96.67)	ppbB	CDS	2E-04	1E-04	45.92	9.34	831.41	3.70	1.03	0.49	0.05	I	V
777345	A (58.59)	G (96.67)	karG	CDS	3E-04	1E-04	40.71	8.29	736.79	3.59	1.03	0.47	0.04	Y	H
156982	C (51.54)	T (90.00)	oppA_1	CDS	4E-04	1E-04	9.44	3.13	40.92	3.54	0.63	0.43	0.02	V	I
637206	A (56.59)	C (96.67)	scrR	CDS	5E-04	1E-04	36.25	7.39	655.80	3.48	1.03	0.45	0.03	K	Q
157069	A (51.54)	G (86.67)	oppA_1	CDS	7E-04	3E-04	6.81	2.48	24.09	3.39	0.57	0.44	0.02	S	P
367095	C (60.77)	T (73.33)	CTA_0348	CDS	1E-03	1E-03	4.23	1.81	10.82	3.20	0.45	0.46	0.01	T	I
544233	A (61.54)	G (73.33)	CTA_0510	CDS	1E-03	3E-04	4.23	1.81	10.82	3.20	0.45	0.46	0.02	R	G
954865	A (59.69)	G (73.33)	pmpD	CDS	2E-03	1E-04	4.04	1.73	10.33	3.10	0.45	0.46	0.04	E	G
969418	C (59.06)	T (73.33)	sucD	CDS	2E-03	1E-04	3.94	1.68	10.07	3.04	0.45	0.46	0.03	T	I
544610	A (61.54)	G (70.00)	atoS	CDS	3E-03	1E-03	3.59	1.56	8.85	2.92	0.44	0.45	0.01	D	G
543548	T (60.63)	C (70.00)	CTA_0508	CDS	5E-03	1E-04	0.29	0.12	0.67	-2.83	0.44	0.45	0.06	F	S
969583	T (58.73)	C (70.00)	sucD	CDS	7E-03	1E-04	0.30	0.12	0.70	-2.72	0.44	0.46	0.04	L	P
44611	C (60.63)	T (66.67)	CTA_0043	CDS	1E-02	1E-04	2.96	1.30	7.10	2.53	0.43	0.45	0.04	A	V
533906	T (74.62)	C (50.00)	CTA_0498	CDS	1E-02	9E-03	0.35	0.15	0.80	-2.51	0.42	0.31	0.01	L	P
295635	G (61.24)	A (63.33)	CTA_0284	CDS	2E-02	1E-04	0.38	0.16	0.86	-2.30	0.42	0.44	0.03	R	K
95527	C (60.77)	T (60.00)	CTA_0087	CDS	5E-02	4E-02	2.24	1.00	5.15	1.94	0.41	0.44	0.01	S	L
413567	A (60.47)	G (60.00)	CTA_0391	CDS	6E-02	1E-04	2.21	0.99	5.08	1.91	0.41	0.44	0.04	V	A
1027490	G (58.91)	T (60.00)	CTA_0948	CDS	7E-02	1E-04	2.13	0.96	4.91	1.83	0.41	0.45	0.01	P	Q
777183	T (58.59)	C (60.00)	karG	CDS	7E-02	1E-04	0.47	0.21	1.06	-1.80	0.41	0.45	0.04	I	V
168413	A (61.54)	G (93.33)	CTA_0156	CDS	5E-05	1E-04	21.56	6.11	137.2	4.07	0.75	0.50	0.04	H	R
(B)															
SNP position	Reference allele	Alternative allele	Name A/HAR-13	CDS/NCR	Strand	p*	p value	t	SE(t)	OR	95% CI (UL)	(LL)	MAF	N calls at locus	
1028728	C	T	pmpE	CDS	-	0.013	0.011	-2.550	0.555	0.078	0.026	0.232	0.310	7.042	
875804	C	T	aldS	CDS	-	0.024	0.022	-2.298	0.530	0.100	0.036	0.284	0.310	4.225	
939488	G	A	glgA	CDS	-	0.026	0.023	-2.273	0.491	0.103	0.039	0.270	0.479	4.225	
285610	G	A	CTA_0273	CDS	-	0.027	0.034	-2.123	0.526	0.120	0.043	0.336	0.310	4.225	
32779	G	A	trmD	CDS	+	0.032	0.031	-2.160	0.525	0.115	0.041	0.323	0.310	2.817	
465330	C	G	yjfh	CDS	-	0.037	0.042	-2.032	0.519	0.131	0.047	0.362	0.310	1.408	
787841	A	G	NA	inter	NA	0.038	0.038	-2.074	0.524	0.126	0.045	0.351	0.310	4.225	

**Table 2** SNPs across the *Chlamydia trachomatis* genome identified using permutation-based genome-wide association analysis for (A) ocular localization (non-synonymous only) and (B) disease severity (Continued)

827,184	A	G	CTA_0774	CDS	+	0.041	0.043	-2.020	0.516	0.133	0.048	0.365	0.310	1.408
22,049	G	T	<i>ileS</i>	CDS	+	0.057	0.050	-1.962	0.505	0.141	0.052	0.378	0.324	4.225
152,011	G	A	NA	inter	NA	0.058	0.050	-1.964	0.505	0.140	0.052	0.377	0.324	4.225
710,787	A	C	CTA_0675	CDS	-	0.060	0.052	-1.941	0.517	0.144	0.052	0.396	0.310	4.225
19,085	T	C	NA	inter	NA	0.061	0.060	-1.882	0.530	0.152	0.054	0.430	0.296	5.634
388,175	G	A	CTA_0368	CDS	-	0.061	0.059	-1.889	0.524	0.151	0.054	0.422	0.296	1.408
696,782	A	T	<i>rpoD</i>	CDS	-	0.064	0.062	-1.864	0.511	0.155	0.057	0.422	0.310	1.408
286,636	C	T	<i>lgt</i>	CDS	-	0.065	0.061	-1.876	0.511	0.153	0.056	0.417	0.310	0.000
930,453	C	T	<i>murS</i>	CDS	-	0.067	0.061	-1.876	0.511	0.153	0.056	0.417	0.310	0.000
465,525	C	T	CTA_0439	CDS	-	0.067	0.062	-1.865	0.472	0.155	0.061	0.391	0.493	1.408
60,858	G	A	CTA_0057	CDS	-	0.068	0.070	-1.813	0.512	0.163	0.060	0.445	0.310	1.408
835,039	G	A	CTA_0782	CDS	-	0.070	0.061	-1.876	0.511	0.153	0.056	0.417	0.310	0.000
19,005	A	G	NA	inter	NA	0.071	0.071	-1.807	0.525	0.164	0.059	0.459	0.296	2.817
4554	A	G	<i>gatB</i>	CDS	+	0.071	0.070	-1.813	0.512	0.163	0.060	0.445	0.310	1.408
303,590	C	A	<i>murE</i>	CDS	-	0.072	0.061	-1.876	0.511	0.153	0.056	0.417	0.310	0.000
215,130	C	T	<i>gyrA_1</i>	CDS	-	0.072	0.062	-1.864	0.511	0.155	0.057	0.422	0.310	1.408
806,382	C	T	CTA_0761	CDS	+	0.073	0.058	-1.896	0.530	0.150	0.053	0.424	0.296	4.225
778,783	G	A	<i>rff</i>	CDS	-	0.077	0.075	-1.780	0.502	0.169	0.063	0.451	0.324	2.817
136,812	G	A	<i>incF</i>	CDS	+	0.079	0.075	-1.780	0.502	0.169	0.063	0.451	0.324	2.817
169,573	G	A	CTA_0156	CDS	+	0.082	0.077	-1.771	0.523	0.170	0.061	0.474	0.310	9.859
956,953	C	T	<i>pmpD</i>	CDS	+	0.082	0.072	-1.800	0.523	0.165	0.059	0.461	0.296	2.817
44,990	A	G	<i>ruvB</i>	CDS	+	0.087	0.086	-1.718	0.493	0.179	0.068	0.472	0.338	2.817
62,140	G	T	<i>sucA</i>	CDS	+	0.091	0.078	-1.760	0.502	0.172	0.064	0.461	0.324	5.634
542,521	G	A	CTA_0507	CDS	-	0.092	0.090	-1.696	0.494	0.183	0.070	0.483	0.338	2.817
181,019	C	A	CTA_0164	CDS	-	0.095	0.096	-1.666	0.494	0.189	0.072	0.498	0.338	4.225
151,156	C	G	CTA_0140	CDS	-	0.096	0.077	1.770	0.502	0.172	0.064	0.461	0.324	4.225
1,028,728	C	A	<i>pmpE</i>	CDS	-	0.01	0.011	-2.550	0.555	0.08	0.03	0.23	0.31	13.58%
1,028,728	C	T	<i>pmpE</i>	CDS	-	0.0134	0.0108	-2.5504	0.5550	0.0781	0.0263	0.2317	0.3099	7.0423
875,804	C	T	<i>aldS</i>	CDS	-	0.0242	0.0216	-2.2981	0.5295	0.1005	0.0356	0.2836	0.3099	4.2254
939,488	G	A	<i>glgA</i>	CDS	-	0.0259	0.0230	-2.2727	0.4906	0.1030	0.0394	0.2695	0.4789	4.2254
285,610	G	A	CTA_0273	CDS	-	0.0269	0.0338	-2.1226	0.5264	0.1197	0.0427	0.3359	0.3099	4.2254
32,779	G	A	<i>trmD</i>	CDS	+	0.0318	0.0308	-2.1596	0.5248	0.1154	0.0412	0.3227	0.3099	2.8169
465,330	C	G	<i>yjH</i>	CDS	-	0.0370	0.0422	-2.0315	0.5187	0.1311	0.0474	0.3625	0.3099	1.4085

**Table 2** SNPs across the *Chlamydia trachomatis* genome identified using permutation-based genome-wide association analysis for (A) ocular localization (non-synonymous only) and (B) disease severity (Continued)

787,841	A	G	NA	inter	NA	0.0377	0.0381	-2.0742	0.5236	0.1257	0.0450	0.3506	0.3099	4.2254
827,184	A	G	<i>CTA_0774</i>	CDS	+	0.0413	0.0433	-2.0203	0.5164	0.1326	0.0482	0.3648	0.3099	1.4085
22,049	G	T	<i>ileS</i>	CDS	+	0.0568	0.0497	-1.9624	0.5052	0.1405	0.0522	0.3782	0.3239	4.2254
152,011	G	A	NA	inter	NA	0.0578	0.0495	-1.9642	0.5051	0.1403	0.0521	0.3775	0.3239	4.2254
710,787	A	C	<i>CTA_0675</i>	CDS	-	0.0605	0.0523	-1.9409	0.5174	0.1436	0.0521	0.3958	0.3099	4.2254
19,085	T	C	NA	inter	NA	0.0608	0.0598	-1.8819	0.5298	0.1523	0.0539	0.4302	0.2958	5.6338
388,175	G	A	<i>CTA_0368</i>	CDS	-	0.0610	0.0589	-1.8889	0.5238	0.1512	0.0542	0.4222	0.2958	1.4085
696,782	A	T	<i>rpoD</i>	CDS	-	0.0638	0.0623	-1.8643	0.5114	0.1550	0.0569	0.4223	0.3099	1.4085
286,636	C	T	<i>igt</i>	CDS	-	0.0654	0.0606	-1.8764	0.5113	0.1531	0.0562	0.4172	0.3099	0.0000
930,453	C	T	<i>mus</i>	CDS	-	0.0668	0.0606	-1.8764	0.5113	0.1531	0.0562	0.4172	0.3099	0.0000
465,525	C	T	<i>CTA_0439</i>	CDS	-	0.0670	0.0622	-1.8650	0.4719	0.1549	0.0614	0.3905	0.4930	1.4085
60,858	G	A	<i>CTA_0057</i>	CDS	-	0.0684	0.0698	-1.8134	0.5121	0.1631	0.0598	0.4450	0.3099	1.4085
835,039	G	A	<i>CTA_0782</i>	CDS	-	0.0700	0.0606	-1.8764	0.5113	0.1531	0.0562	0.4172	0.3099	0.0000
19,005	A	G	NA	inter	NA	0.0710	0.0707	-1.8074	0.5254	0.1641	0.0586	0.4595	0.2958	2.8169
4554	A	G	<i>gatB</i>	CDS	+	0.0713	0.0698	-1.8134	0.5121	0.1631	0.0598	0.4450	0.3099	1.4085
303,590	C	A	<i>murE</i>	CDS	-	0.0718	0.0606	-1.8764	0.5113	0.1531	0.0562	0.4172	0.3099	0.0000
215,130	C	T	<i>gyrA_1</i>	CDS	-	0.0722	0.0623	-1.8643	0.5114	0.1550	0.0569	0.4223	0.3099	1.4085
806,382	C	T	<i>CTA_0761</i>	CDS	+	0.0726	0.0580	-1.8960	0.5297	0.1502	0.0532	0.4241	0.2958	4.2254
778,783	G	A	<i>rff</i>	CDS	-	0.0767	0.0751	-1.7797	0.5021	0.1687	0.0630	0.4514	0.3239	2.8169
136,812	G	A	<i>incF</i>	CDS	+	0.0792	0.0751	-1.7797	0.5021	0.1687	0.0630	0.4514	0.3239	2.8169
169,573	G	A	<i>CTA_0156</i>	CDS	+	0.0821	0.0765	-1.7712	0.5227	0.1701	0.0611	0.4740	0.3099	9.8592
956,953	C	T	<i>pmpD</i>	CDS	+	0.0823	0.0719	-1.7998	0.5226	0.1653	0.0594	0.4605	0.2958	2.8169
44,990	A	G	<i>ruvB</i>	CDS	+	0.0871	0.0858	-1.7181	0.4932	0.1794	0.0682	0.4717	0.3380	2.8169
62,140	G	T	<i>sucA</i>	CDS	+	0.0914	0.0784	-1.7601	0.5024	0.1720	0.0643	0.4605	0.3239	5.6338
542,521	G	A	<i>CTA_0507</i>	CDS	-	0.0916	0.0899	-1.6960	0.4940	0.1834	0.0696	0.4830	0.3380	2.8169
181,019	C	A	<i>CTA_0164</i>	CDS	-	0.0953	0.0958	-1.6656	0.4940	0.1891	0.0718	0.4979	0.3380	4.2254
151,156	C	G	<i>CTA_0140</i>	CDS	-	0.0955	0.0767	1.7701	0.5019	0.1701	0.0611	0.4740	0.3099	9.8592

(a) Ocular localization-associated non-synonymous SNPs ( $p$  value < 0.1). Position of the SNPs and name of the impacted gene are from the Cr A/HAR-13 (GenBank accession number NC\_007429) genome. 'Allele percentage' is the percentage of each group where the given allele was present. 'CDS/NCR' identifies whether the SNP was in a coding or non-coding region.  $p^*$  indicates  $p$  values from 100,024 simulations indicating genome-wide significance at  $p^* < 0.05$ . 'r' is the  $t$  statistic; SE(r) is the standard error of the  $t$  statistic. 'OR' is the adjusted odds ratio (derived from the  $t$  statistic). '95% CI' = 95% confidence interval of the OR; 'UL' upper limit; 'LL' lower limit. 'MAF' is the minor allele frequency. 'N calls at locus' is the proportion of isolates which had no base called. 'AA' is the amino acid coded for

(b) Disease severity-associated SNPs ( $p$  value < 0.1). Disease severity is defined by a composite in vivo conjunctival phenotype derived using principal component analysis using ocular *C. trachomatis* load and conjunctival inflammatory (P) score (using the modified FPC (follicles, papillary hypertrophy, conjunctival scarring) trachoma grading system [39]). Reference allele indicates the reference allele on Cr A/HAR-13 (GenBank accession number NC\_007429). 'CDS/NCR' identifies whether the SNP was in a coding, non-coding or intergenic region.  $p^*$  = permuted  $p$  value after 100,024 simulations indicating genome-wide significance at  $p^* < 0.05$ . 'r' is the  $t$  statistic; SE(r) is the standard error of the  $t$  statistic. 'OR' is the adjusted odds ratio (derived from the  $t$  statistic). '95% CI' = 95% confidence interval of the OR; 'UL' upper limit; 'LL' lower limit. 'MAF' is the minor allele frequency. 'N calls at locus' is the proportion of isolates which had no base called

The apparent village-level clustering provides new evidence that WGS has the necessary molecular resolution to fully investigate *Ct* transmission. Although the number of sequences from each village was very small, overall *Ct* genomic diversity supports our hypothesis of ongoing or recent transmission, since diversity requires mutation, recombination and gene flow. The data from this study demonstrate such mutation and indicate that WGS data may be useful in defining transmission networks and developing transmission maps, which have not been adequately defined using alternative *Ct* genotyping systems. Whole genome mapping has previously been shown to be a useful tool in the analysis of outbreaks and bacterial pathogen transmission [80, 81] and thus has multiple potential applications in epidemiological analysis and transmission studies. However, greater numbers of sequences per village are required to validate this finding.

Such diversity is likely to be representative of recombination present in *Ct* [82]. Genome-wide recombination was common and widespread within these sequences. Extensive recombination has been noted in previous studies and is thought to be a source of diversification with possible interstrain recombination [4, 82]. Recombination may represent fixation of recombination in regions that are under diversifying selection pressure [4].

Recently, a handful of bacterial GWASs have provided insight into the genetic basis of bacterial host preference, antibiotic resistance and virulence [83–88]. Until now, most inferences regarding disease-modifying virulence factors in chlamydial infection have been derived from a limited number of comparative genomic studies where only a few virulence factors were associated with disease severity. Chlamydial genomic association data have previously been used to highlight genes potentially involved in pathoadaptation [10, 89] and tissue localization [90].

In the current GWAS we found 21 genome-wide significant non-synonymous SNPs associated with ocular localization and eight genome-wide significant synonymous SNPs associated with disease severity.

Confidence that new SNPs identified in the ocular localization GWAS are candidate markers of pathoadaptation is supported by the observation that half of the SNPs identified have previously been described as polymorphic or recombinant within *Ct* and the ocular serovars [8, 91–93].

In support of the hypothesis that early events in infection and intracellular growth are crucial events in *Ct* survival and pathogenicity, we identified SNPs within genes that are expressed from the beginning of the chlamydial developmental cycle including *CTA0156* (encoding early endosomal antigen 1 (EEA1) [73]), *CTA0498* (encoding translocated actin-recruiting phosphoprotein (*tarP*) [94]) and *CTA0884* (encoding polymorphic membrane protein D (PmpD) [95]), which have identified roles in entry to and initial interactions with host cells.

Two of the four genes containing multiple non-synonymous SNPs (*karG* and *sucD*) are involved in ATP metabolism and, more generally, chlamydial metabolism. Two of the genes with multiple synonymous mutations (*ruvB* and *CTA\_0284*) are also involved in metabolism. Growth rates are known to vary significantly between biovars. The developmental cycle in ocular serovars is substantially longer than that in genital serovars [96]. These genes and the identified SNPs may therefore be important in the differential growth and development of *Ct* serovars. This is supported by the downregulation of *sucD* expression during in vitro persistence. Slower growth in ocular strains occurs primarily in the entry and early stages of differentiation, which may also indicate the role of previously described genes involved in entry into cells.

The eight disease severity-associated SNPs are within less well-characterized genes. Apart from *pmpE*, the remaining genes identified in this study have been shown to be relatively conserved [90]. This suggests that these SNPs may be important in ocular *Ct* pathogenesis, rather than in longer term chlamydial evolution. Three of these genes are putative *Ct* virulence factors, with functions in nutrient acquisition (*glgA* [24, 28, 97]), host-cell adhesion (*pmpE* [98]) and response to IFN $\gamma$ -induced stress (*trmD* [73]). Homologues of *alaS* [99, 100] and *CTA0273* [101, 102] are known virulence factors in related Gram-negative bacteria, suggesting that these genes are potentially important in *Ct* pathogenesis.

Transcriptome analysis of chlamydial growth in vitro has shown that there is highly upregulated gene expression of *trmD* (encoding a transfer RNA (tRNA) methyltransferase) associated with growth in the presence of IFN $\gamma$ , thought to be important in the maintenance of chlamydial infection [73]. *yjfH* (renamed *rlmB*) is phylogenetically related to the TrmD family and encodes the protein RlmB, which is important for the synthesis and assembly of the components of the ribosome [103]. In *Escherichia coli*, *Haemophilus influenzae* and *Mycoplasma genitalium*, RlmB catalyses the methylation of guanosine 2251 in 23S ribosomal RNA (rRNA), which is of importance in peptidyl tRNA recognition but is not essential for bacterial growth [103, 104]. *alaS* encodes a tRNA ligase of the class II aminoacyl tRNA synthetase family involved in cytoplasmic protein biosynthesis. It is not known to have virulence associations in chlamydial infection, but has been described as a component of a virulence operon in *Haemophilus ducreyi* [99] and *H. influenzae* [100]. The CDS *CTA0273* encodes a predicted inner membrane protein translocase component of the autotransporter YidC, an inner membrane

insertase important in virulence in *E. coli* [101] and *Streptococcus mutans* [102]. Our study suggests that these loci may be important in disease severity and host-pathogen interactions in chlamydial infection. A summary of available literature for these key ocular localization and disease severity-associated SNPs is tabulated in Additional file 11: Figure S11. We cannot speculate further on the effect of these polymorphisms on expression. It is possible that the synonymous disease severity-associated SNPs are markers in linkage for disease-causing alleles that were not included in the final GWAS analysis. For both analyses, further mechanistic studies are required to establish causality and validity and to fully understand the nature of the associations presented.

Though we were intrinsically limited to those cases where infection was detectable and from which we were able to obtain *Ct* WGS data, our population-based treatment-naïve sample attempts to provide a representative picture of what is observed in ocular *Ct* infection. We acknowledge that there may be *Ct* genotypes that are cleared by the immune system such that we do not capture them in a cross-sectional study. We are limited to the small sample size in this study, but attempt to address the issues of statistical power and multiple testing by using a bi-dimensional conjunctival phenotype and permutation-based multi-variable regression analysis. To date, many published microbial GWASs have sample sizes under 500 [105], including several key studies examining virulence [84] and drug resistance [85] in *Staphylococcus aureus* with sample sizes of 75 and 90 respectively.

## Conclusions

The potential of bacterial GWASs has only recently been realized, and despite the limitations with sample size, their use to study *Ct* in this way is particularly important, since in vitro models are intrinsically difficult to develop, and it has not been possible to study urogenital *Ct* in the same way due to the lack of a clearly defined in vivo disease phenotype. The genomic markers identified in this study provide important direction for validation through in vitro functional studies and a unique opportunity to understand host-pathogen interactions likely to be important in *Ct* pathogenesis in humans. The greater than expected diversity within this population of naturally circulating ocular *Ct* and the clustering at village level demonstrate the potential utility of WGS in epidemiological and clinical studies. This will enable us to understand transmission in both ocular and urogenital *Ct* infection and will have significant public health implications in preventing and eliminating chlamydial disease in humans.

## Additional files

**Additional file 1: Figure S1.** Histogram and density plot showing log-transformed *C. trachomatis* load (*omcB* copies/swab) data. (PDF 111 kb)

**Additional file 2: Figure S2.** Detailed summary of whole genome sequence (WGS) data quality control of Bijagós *Chlamydia trachomatis* sequences. (PDF 76 kb)

**Additional file 3: Figure S3.** R Script used for (A) tissue localization and (B) disease severity *Chlamydia trachomatis* GWAS. (PDF 180 kb)

**Additional file 4: Figure S4.** Maximum likelihood reconstruction of whole genome phylogeny of *Chlamydia trachomatis* sequences examined in the tissue localization analysis. (PDF 357 kb)

**Additional file 5: Figure S5.** Maximum likelihood reconstruction of the *ompA* (CTA0742) phylogeny. (PDF 450 kb)

**Additional file 6: Figure S6.** Recombination present across Bijagós *Chlamydia trachomatis* genome sequences using the pairwise homoplasy index (Phi) and the site-wise log likelihood support for the best-scoring maximum likelihood tree. (PDF 153 kb)

**Additional file 7: Figure S7.** Tyrosine repeat regions and actin-binding domains in *tarP* (CTA0948) and polymorphisms in the *trp* operon (CTA0182–CTA0186) (*trpR*, *trpB* and *trpA*) within Bijagós (Bissau-Guinean) ocular *Chlamydia trachomatis* sequences. (PDF 49 kb)

**Additional file 8: Figure S8.** Maximum likelihood reconstruction of phylogeny by polymorphic membrane protein (Pmp) genes A–I. (PDF 1738 kb)

**Additional file 9: Figure S9.** Ocular localization-associated SNPs ( $p$  value < 0.1). (PDF 150 kb)

**Additional file 10: Figure S10.** SNPs across the *Chlamydia trachomatis* genome associated with disease severity using permutation-based genome-wide association analysis. (PDF 158 kb)

**Additional file 11: Figure S11.** Summary of published studies supporting the key ocular localization and disease severity-associated SNPs [106–114]. (PDF 105 kb)

**Additional file 12: Figure S12.** European Nucleotide Archive (ENA) (European Bioinformatics Institute (EBI)) accession numbers relating to *C. trachomatis* sequence data analysed in this study. (PDF 75 kb)

## Abbreviations

ATP: Adenosine triphosphate; *Ct*: *Chlamydia trachomatis*; ddPCR: Droplet digital PCR; DMEM: Dulbecco's modified Eagle's medium; DNA: Deoxyribonucleic acid; EB: Elementary body; FPC: Follides, papillary hypertrophy, conjunctival scarring; GWAS: Genome-wide association study; indels: Insertions and deletions; LGV: Lymphogranuloma venereum; MAF: Minor allele frequency; MOMP: Major outer membrane protein; NHP: Non-human primate; NSS: Neighbour similarity score; PC: Principal component; PCA: Principal component analysis; PCR: Polymerase chain reaction; SNP: Single nucleotide polymorphism; WGS: Whole genome sequencing

## Acknowledgements

We extend thanks to colleagues at the Programa Nacional de Saúde de Visão in the Ministério de Saúde Pública in Bissau, the study participants and dedicated field research team in Guinea-Bissau and the Medical Research Council (MRC) Unit The Gambia for their support and collaboration in this work.

## Funding

ARL was funded by the Wellcome Trust through a Clinical Research Training Fellowship (grant number 097330/Z/11/Z). MJH and ChR were funded by a Wellcome Trust Program Grant (grant number 079246/Z/06/Z). ChR was funded by the Wellcome Trust Institutional Strategic Support Fund (grant number 105609/Z/14/Z). Work undertaken by the Wellcome Trust Sanger Institute by NRT, HSS and JH was supported by the Wellcome Trust (grant number 098051) and the Wellcome Trust Institutional Strategic Support Fund (grant number 105609/Z/14/Z). TGC is funded by the MRC UK (grant numbers MR/K000551/1, MR/M01360X/1, MR/N010469/1). JP was funded by a Biotechnology and Biological Sciences Research Council (BBSRC) PhD studentship, and FC and HP were funded by Bloomsbury Colleges Research Fund PhD studentships.



#### Availability of data and materials

All sequence data are available from the European Bioinformatics Institute (EBI) short read archive. See Additional file 12: Figure S12 for details and accession numbers.

#### Authors' contributions

ARL, RLB, MJH, SEB and NRT designed the study. ARL, SEB, EC and MN conducted the field study. ARL, ChR and SEB conducted the molecular laboratory work. LTC and INC performed the chlamydial cell culture. HSS and JH designed and performed the whole genome sequencing and initial FastQC. ARL, ChR, HP, FC and TGC conducted the GWAS analysis. HP, JP, SH, JH and HSS supported the phylogenetic analysis. ARL, HP, MJH, DCWM, TGC and NRT wrote the paper. All authors have contributed to and reviewed the manuscript. All authors read and approved the final manuscript.

#### Ethics approval and consent to participate

This study was conducted in accordance with the declaration of Helsinki. Ethical approval was obtained from the Comité Nacional de Ética e Saúde (Guinea-Bissau), the London School of Hygiene and Tropical Medicine Ethics Committee (UK) and The Gambia Government/MRC Joint Ethics Committee (The Gambia). Written informed consent to participate and publish anonymized patient data was obtained from all study participants or their guardians on their behalf if participants were children. A signature or thumbprint was considered an appropriate record of consent in this setting by the above ethical bodies. All communities received treatment for endemic trachoma in accordance with the World Health Organization and national policies following the survey.

#### Consent for publication

Written informed consent to publish anonymized patient data was obtained from all study participants as described above.

#### Competing interests

The authors declare that they have no competing interests.

#### Publisher's Note

Springer Nature remains neutral with regard to jurisdictional claims in published maps and institutional affiliations.

#### Author details

<sup>1</sup>Clinical Research Department, London School of Hygiene and Tropical Medicine, Keppel Street, London, UK. <sup>2</sup>Department of Pathogen Molecular Biology, London School of Hygiene and Tropical Medicine, Keppel Street, London, UK. <sup>3</sup>Disease Control and Elimination Theme, Medical Research Council Unit The Gambia, Fajara, Gambia. <sup>4</sup>Programa Nacional de Saúde de Visão, Ministério de Saúde Pública, Bissau, Guinea-Bissau. <sup>5</sup>Pathogen Genomics, Wellcome Trust Sanger Institute, Wellcome Trust Genome Campus, Hinxton, UK. <sup>6</sup>Clinical Microbiology, Universitätsspital Basel, Basel, Switzerland. <sup>7</sup>Applied Microbiology Research, Department of Biomedicine, University of Basel, Basel, Switzerland. <sup>8</sup>Molecular Microbiology Group, University of Southampton Medical School, Southampton, UK. <sup>9</sup>Department of Infectious Diseases Epidemiology, London School of Hygiene and Tropical Medicine, Keppel Street, London, UK.

Received: 14 October 2017 Accepted: 13 February 2018

Published online: 26 February 2018

#### References

- Hu VH, et al. Epidemiology and control of trachoma: systematic review. *Tropical Med Int Health*. 2010;15(6):673–91.
- World Health Organization. Sexually transmitted infections (STIs); 2016. <http://www.who.int/mediacentre/factsheets/fs110/en/>.
- Rodriguez P, et al. Typing of *Chlamydia trachomatis* by restriction endonuclease analysis of the amplified major outer membrane protein gene. *J Clin Microbiol*. 1991;29:1132–6.
- Harris SR, et al. Whole genome analysis of diverse *Chlamydia trachomatis* strains identifies phylogenetic relationships masked by current clinical typing. *Nat Genet*. 2012;44(4):413–s1.
- Caldwell HD, et al. Polymorphisms in *Chlamydia trachomatis* tryptophan synthase genes differentiates between genital and ocular isolates: implications in pathogenesis and infection tropism. *J Clin Invest*. 2003; 111:1757–69.
- Jeffrey BM, et al. Genome sequencing of recent clinical *Chlamydia trachomatis* strains identifies loci associated with tissue tropism and regions of apparent recombination. *Infect Immun*. 2010;78:2544–53.
- Nunes A, Borrego MJ, Gomes JP. Genomic features beyond *C. trachomatis* phenotypes: what do we think we know? *Infect Genet Evol*. 2013;16:392–400.
- Kari L, et al. Pathogenic diversity among *Chlamydia trachomatis* ocular strains in non-human primates is affected by subtle genomic variations. *J Infect Dis*. 2008;197:449–56.
- Butcher RMR, et al. Low prevalence of conjunctival infection with *Chlamydia trachomatis* in a treatment-naive trachoma-endemic region of the Solomon Islands. *PLoS Negl Trop Dis*. 2016;10(10):e0005051.
- Andersson P, et al. *Chlamydia trachomatis* from Australian Aboriginal people with trachoma are polyphyletic composed of multiple distinctive lineages. *Nat Commun*. 2016;7:10688.
- Feng L, et al. Survey, culture and genome analysis of ocular *Chlamydia trachomatis* in Tibetan boarding primary schools in Qinghai Province, China. *Front Cell Infect Microbiol*. 2017;6:207.
- Borges V, et al. Complete genome sequence of *Chlamydia trachomatis* ocular serovar C strain TW-3. *Genome Announc*. 2014;2:e01204–13.
- Darville T, Hiltke T. Pathogenesis of genital tract disease due to *Chlamydia trachomatis*. *J Infect Dis*. 2010;201(Supplement\_2):S114–225.
- van Valkengoed IG, et al. Overestimation of complication rates in evaluations of *Chlamydia trachomatis* screening programmes—implications for cost-effectiveness analyses. *Int J Epidemiol*. 2004;33(2):416–25.
- Bailey RL, et al. Molecular epidemiology of trachoma in a Gambian village. *Br J Ophthalmol*. 1994;78:813–7.
- Andreasen AA, et al. *Chlamydia trachomatis* ompA variants in trachoma: what do they tell us? *PLoS Negl Trop Dis*. 2008;2(9):e306.
- Wang Y, et al. Development of a transformation system for *Chlamydia trachomatis*: restoration of glycogen biosynthesis by acquisition of a plasmid shuttle vector. *PLoS Pathog*. 2011;7(9):e1002258.
- Wang Y, et al. Transformation of a plasmid-free genital tract isolate with a plasmid vector carrying a deletion in CDS6 revealed that this gene regulates inclusion phenotype. *Pathogens Dis*. 2013;67(2):100–3.
- Longbottom D, et al. Molecular cloning and characterization of genes coding for the highly immunogenic cluster of 90 kilodalton envelope proteins from the *Chlamydia psittaci* subtype that causes abortion in sheep. *Infect Immun*. 1998;66:1317–24.
- Gomes JP, et al. Polymorphisms in the nine polymorphic membrane proteins of *Chlamydia trachomatis* across all serovars: evidence for serovar Da recombination and correlation with tissue tropism. *J Bacteriol*. 2006;188:275–86.
- Rockey DD, Heinzen RA, Hackstadt T. Cloning and characterization of a *Chlamydia psittaci* gene coding for a protein localized in the inclusion membrane of infected cells. *Mol Microbiol*. 1995;15:617–26.
- Hefty PS, Stephens RS. *Chlamydia trachomatis* type III secretion system is encoded on ten operons preceded by a sigma 70-like promoter element. *J Bacteriol*. 2007;189:198–206.
- Carlson JH, et al. *In vivo* and *in vitro* studies of *Chlamydia trachomatis* TrpR: DNA interaction. *Mol Microbiol*. 2006;59(6):1678–91.
- O'Connell CM, et al. Toll-like receptor 2 activation by *Chlamydia trachomatis* is plasmid dependent, and plasmid-responsive chromosomal loci are coordinately regulated in response to glucose limitation by *C. trachomatis* but not by *C. muridarum*. *Infect Immun*. 2011;79:1044–56.
- Hackstadt T, Scidmore-Carlson MA, Shaw EI, Fischer ER. *Chlamydia trachomatis* IncA protein is required for homotypic vesicle fusion. *Cell Microbiol*. 1999;1:119–30.
- Nelson DE, et al. Inhibition of Chlamydiae by primary alcohols correlates with strain specific complement of plasticity zone phospholipase D genes. *Infect Immun*. 2006;74(1):73–80.
- Carlson JH, Hughes S, Hogan D. Polymorphisms in the *Chlamydia trachomatis* cytotoxin locus associated with ocular and genital isolates. *Infect Immun*. 2004;72(12):7063–72.
- Carlson JH, et al. The *Chlamydia trachomatis* plasmid is a transcriptional regulator of chromosomal genes and a virulence factor. *Infect Immun*. 2008;76:2273–83.
- Frazer LC, et al. Plasmid-cured *Chlamydia caviae* activates TLR2-dependent signaling and retains virulence in the guinea pig model of genital tract infection. *PLoS One*. 2012;7(1):e30747.
- Song L, et al. *Chlamydia trachomatis* plasmid-encoded *ppg4* is a transcriptional regulator of virulence-associated genes. *Infect Immun*. 2013;81(3):636.

31. Christiansen MT, et al. Whole genome enrichment and sequencing of *Chlamydia trachomatis* directly from clinical samples. *BMC Infect Dis.* 2014;14:591.
32. Borges V, et al. Effect of long-term laboratory propagation on *Chlamydia trachomatis* genome dynamics. *Infect Genet Evol.* 2013;17:23–32.
33. Borges V, et al. *Chlamydia trachomatis* *in vivo* to *in vitro* transition reveals mechanisms of phase variation and downregulation of virulence factors. *PLoS One.* 2015;10(7):e0133420.
34. Bonner C, et al. *Chlamydia trachomatis* virulence factor CT135 is stable *in vivo* but highly polymorphic *in vitro*. *Pathog Dis.* 2015;73(6):ftv043.
35. Burton MJ, et al. Which members of a community need antibiotics to control trachoma? Conjunctival *Chlamydia trachomatis* load in Gambian villages. *Invest Ophthalmol Vis Sci.* 2003;44(10):4215–22.
36. Conway DJ, et al. Scarring trachoma is associated with polymorphisms in TNF-alpha gene promoter and with increased TNF-alpha levels in tear fluid. *Infect Immun.* 1997;65(3):1003–6.
37. West SK, et al. Progression of active trachoma to scarring in a cohort of Tanzanian children. *Ophthalmic Epidemiol.* 2001;8(2–3):137–44.
38. Burton MJ, et al. Pathogenesis of progressive scarring trachoma in Ethiopia and Tanzania: two cohort studies. *PLoS Negl Trop Dis.* 2015;9(5):e0003763.
39. Dawson CR, Jones BR, Tarizzo ML. Guide to trachoma control in programs for the prevention of blindness. Geneva: World Health Organization; 1981.
40. Reid JS, et al. A principal component meta-analysis on multiple anthropometric traits identifies novel loci for body shape. *Nat Comms.* 2016;7:13357.
41. Yang J, et al. Conditional and joint multiple SNP analysis of GWAS summary statistics identifies additional variance influencing complex traits. *Nat Genet.* 2012;44:51–3.
42. Aschard H, et al. Maximising the power of principal component analysis of correlated phenotypes in genome wide association studies. *Am J Hum Genet.* 2014;94:662–76.
43. Last AR, et al. Risk factors for active trachoma and ocular *Chlamydia trachomatis* infection in treatment-naïve trachoma-hyperendemic communities of the Bijagós Archipelago, Guinea Bissau. *PLoS Negl Trop Dis.* 2014;8(6):e2900.
44. Last A, et al. Plasmid copy number and disease severity in naturally occurring ocular *Chlamydia trachomatis* infection. *J Clin Microbiol.* 2014; 52(1):324–7.
45. Roberts C, et al. Development and evaluation of a next generation digital PCR diagnostic assay for ocular *Chlamydia trachomatis* infections. *J Clin Microbiol.* 2013;51(7):2195–203.
46. Burton MJ, et al. Conjunctival chlamydial 16S ribosomal RNA expression in trachoma: is chlamydial metabolic activity required for disease to develop? *Clin Infect Dis.* 2006;42:463–70.
47. Faal N, et al. Conjunctival FOXP3 expression in trachoma: do regulatory T cells have a role in human ocular *Chlamydia trachomatis* infection? *PLoS Med.* 2006;3(8):e266.
48. Derrick T, et al. Inverse relationship between micro RNA-155 and -184 expression with increasing conjunctival inflammation during ocular *Chlamydia trachomatis* infection. *BMC Infect Dis.* 2016;16:60.
49. Last A, et al. Spatial clustering of high load ocular *Chlamydia trachomatis* infection in trachoma: a cross-sectional population-based study. *Pathog Dis.* 2017;75(5) <https://doi.org/10.1093/femspd/ftx050>.
50. Suo C, et al. Analysis of multiple phenotypes in genome wide genetic mapping studies. *BMC Bioinformatics.* 2013;14:151.
51. Skipp P, Robinson J, O'Connor CD, Clarke IN. Shotgun proteomic analysis of *Chlamydia trachomatis*. *Proteomics.* 2005;5(6):1558–73.
52. Seth-Smith HMB, et al. Co-evolution of genomes and plasmids within *Chlamydia trachomatis* and the emergence in Sweden of a new variant strain. *BMC Genomics.* 2009;10:239.
53. Andrews S. FastQC: a quality control tool for high throughput sequence data; 2010. <http://www.bioinformatics.babraham.ac.uk/projects/fastqc>.
54. Langmead B, et al. Ultrafast and memory-efficient alignment of short DNA sequences to the human genome. *Genome Biol.* 2009;10:R25.3.
55. Li H, et al. The sequence alignment/map format and SAMtools. *Bioinformatics.* 2009;25:2078–9.
56. McKenna A, et al. The Genome Analysis Tool Kit: a MapReduce framework for analysing next generation DNA sequencing data. *Genome Res.* 2010;20:1297–303.
57. Cheng AY, Teo YY, Ong RT. Assessing single nucleotide variant detection and genotype calling on whole genome sequenced individuals. *Bioinformatics.* 2014;30(12):1707–13.
58. Gudbjartsson DF, et al. Large-scale whole genome sequencing of the Icelandic population. *Nat Genet.* 2015;47(5):435–44.
59. Pickering H, et al. Genome-wide profiling of humoral immunity and pathogen genes under selection identifies immune evasion tactics of *Chlamydia trachomatis* during ocular infection. *Sci Rep.* 2017;7(1):9634.
60. Coll F, et al. PolyTB: a genomic variation map for *Mycobacterium tuberculosis*. *Tuberculosis (Edinb).* 2014;94(3):346–54.
61. Hadfield J, et al. Comprehensive global genome dynamics of *Chlamydia trachomatis* show ancient diversification followed by contemporary mixing and recent lineage expansion. *Genome Res.* 2017;27:1–10.
62. Stamatakis A, Hoover P, Rougemont J. A rapid bootstrap algorithm for the RAxML Web servers. *Syst Biol.* 2008;57:758–71.
63. Bruen TC, Philippe H, Bryant D. A simple and robust statistical test for detecting the presence of recombination. *Genetics.* 2006;172:2665–81.
64. Solomon AW, et al. Strategies for control of trachoma: observational study with quantitative PCR. *Lancet.* 2003;362(9379):198–204.
65. Gouy M, Guindon S, Gascuel O. SeaView version 4: a multiplatform graphical user interface for sequence alignment and phylogenetic tree building. *Mol Biol Evol.* 2010;27(2):221–114.
66. Heger A, Holm L. Rapid automatic detection and alignment of repeats in protein sequences. *Proteins.* 2000;41(2):224–37.
67. Sonnhammer EL, Eddy SR, Durbin R. Pfam: a comprehensive database of protein domain families based on seed alignments. *Proteins.* 1997;28(3):405–20.
68. Nei M, Masatoshi N, Wen-Hsiung L. Mathematical model for studying genetic variation in terms of restriction endonucleases. *Proc Natl Acad Sci.* 1979;76(10):5269–73.
69. Che R, et al. An adaptive permutation approach for genome-wide association study. *BioData Mining.* 2014;7:9.
70. Dudoit S, et al. Multiple hypothesis testing in microarray experiments. *Stat Sci.* 2003;18(1):71–103.
71. Sham PC, Purcell SM. Statistical power and significance testing in large scale genetic studies. *Nat Rev Genet.* 2014;15(5):335–46.
72. Fairfax BP, et al. Genetics of gene expression in primary immune cells identifies cell type-specific master regulators and roles of HLA alleles. *Nat Genet.* 2012;44(5):502–10.
73. Belland RJ, et al. Genomic transcriptional profiling of the developmental cycle of *Chlamydia trachomatis*. *Proc Natl Acad Sci U S A.* 2003;100(14): 8478–83.
74. Yu GS, Lin CJ, Hwang JK. Predicting subcellular localization of proteins for Gram-negative bacterial by support vector machines based on n-peptide compositions. *Protein Sci.* 2004;13(5):1402–6.
75. Yu NY, et al. PSORTb 3.0: improved protein subcellular localization prediction with refined localization subcategories and predictive capabilities for all prokaryotes. *Bioinformatics.* 2010;26(13):1608–15.
76. Goldberg T, et al. LocTree3 prediction of localization. *Nucleic Acids Res.* 2014;42(Web Server Issue):W350–5.
77. Thomas A, et al. Effect of linkage disequilibrium on the identification of functional variants. *Genet Epidemiol.* 2011;35(Suppl 1):S115–9.
78. Lutter EI, et al. Phylogenetic analysis of *Chlamydia trachomatis* TARP and correlation with clinical phenotype. *Infect Immun.* 2010;78(9):3678–88.
79. Pepperell CS, et al. The role of selection in shaping diversity of natural *Mycobacterium tuberculosis* populations. *PLoS Pathog.* 2013;9(8):10.1371.
80. Fey PD, et al. Assessment of whole genome mapping in a well-defined outbreak of *Salmonella enterica* serotype Saintpaul. *J Clin Microbiol.* 2012; 50(9):3063–5.
81. Gilchrist CA, Turner SD, Riley MF, Petri WA Jr, Hewlett EL. Whole genome sequencing in outbreak analysis. *Clin Microbiol Rev.* 2015;28(3):541–63.
82. Gomes JP, et al. Evolution of *Chlamydia trachomatis* diversity occurs by widespread interstrain recombination involving hotspots. *Genome Res.* 2007;17(1):50–60.
83. Sheppard SK, et al. Genome-wide association study identifies vitamin B5 biosynthesis as a host specificity factor in *Campylobacter*. *Proc Natl Acad Sci U S A.* 2013;110:11923–7.
84. Laabei M, et al. Predicting the virulence of MRSA from its genome sequence. *Genome Res.* 2014;24(5):839–49.
85. Alam MT, et al. Dissecting vancomycin intermediate resistance in *Staphylococcus aureus* using genome-wide association. *Genome Biol Evol.* 2014;6:1174–85.
86. Chewapreecha C, et al. Comprehensive identification of single nucleotide polymorphisms associated with beta-lactam resistance within pneumococcal mosaic genes. *PLoS Genet.* 2014;10:e1004547.
87. Maury M, et al. Uncovering *Listeria monocytogenes* hypervirulence by harnessing its biodiversity. *Nat Genet.* 2016;48:308–13.

88. Earle SG, et al. Identifying lineage effects when controlling for population structure improves power in bacterial association studies. *Nature Microbiol.* 2016;1:16041.
89. Borges V, Gomes JP. Deep comparative genomics among *Chlamydia trachomatis* lymphogranuloma venereum isolates highlights genes potentially involved in pathoadaptation. *Infect Genet Evol.* 2015;32:74–88.
90. Ferreira R, et al. *In silico* scrutiny of genes revealing phylogenetic congruence with clinical prevalence or tropism properties of *Chlamydia trachomatis* strains. *G3.* 2014;5(1):9–19.
91. Carlson JH, Porcella SF, McClarty G. Comparative genomic analysis of *Chlamydia trachomatis* oculotropic and genitotropic strains. *Infect Immun.* 2005;73(10):6407–18.
92. Brunelle BW, Nicholson TL, Stephens RS. Micro-array based genomic surveying of gene polymorphisms in *Chlamydia trachomatis*. *Genome Biol.* 2004;5(6):R42.
93. Borges V, Nunes A, Ferreira R, Borrego MJ, Gomes JP. Directional evolution of *Chlamydia trachomatis* towards niche-specific adaptation. *J Bacteriol.* 2012;194(22):6143–53.
94. Clifton DR, et al. A Chlamydial type III translocated protein is tyrosine-phosphorylated at the site of entry and associated with the recruitment of actin. *Proc Natl Acad Sci U S A.* 2004;101(27):10166–71.
95. Kari L, et al. *Chlamydia trachomatis* polymorphic membrane protein D is a virulence factor involved in early host-cell interactions. *Infect Immun.* 2014;82(7):2756–62.
96. Miyairi I, et al. Different growth rates of *Chlamydia trachomatis* biovars reflect pathotype. *J Infect Dis.* 2006;194(3):350–7.
97. Da Cunha M, et al. Identification of type THREE secretion substrates of *Chlamydia trachomatis* using *Yersinia enterocolitica* as a heterologous system. *BMC Microbiol.* 2014;17(14):40.
98. Becker E, Hegemann JH. All subtypes of the Pmp adhesion family are implicated in chlamydial virulence and show species-specific function. *Microbiology.* 2014;3(4):544–56.
99. Gangaiah D, et al. Carbon storage regulator A contributes to the virulence of *Haemophilus ducreyi* in humans by multiple mechanisms. *Infect Immun.* 2013;81(2):608–17.
100. Hogg JS, et al. Characterisation and modeling of the *Haemophilus influenzae* core and supragenomes based on the complete genomic sequences of Rd and 12 clinical non-typeable strains. *Genome Biol.* 2007;8:R103.1–8.
101. Samuelson JC, et al. YidC mediates membrane protein insertion in bacteria. *Nature.* 2000;406(6796):637–41.
102. Palmer SR, et al. YidC1 and YidC2 are functionally distinct proteins involved in protein secretion, biofilm formation and cariogenicity of *Streptococcus mutans*. *Microbiology.* 2012;158(7):1702–12.
103. Michel G, et al. The structure of the RlmB 23S rRNA methyltransferase reveals a new methylation fold with a unique knot. *Structure.* 2002;10(10):1303–15.
104. Lovgren JM, Wikstrom PM. The *rlmB* gene is essential for formation of Gm2251 in 23S rRNA but not for ribosome maturation in *Escherichia coli*. *J Bacteriol.* 2001;183(23):6957–60.
105. Power RA, Parkhill J, de Oliveira T. Microbial genome-wide association studies: lessons from human GWAS. *Nat Rev Genet.* 2017;18(1):41–50.
106. Le Negrate G, et al. ChaDub1 of *Chlamydia trachomatis* suppresses NF- $\kappa$ B activation and inhibits 1- $\kappa$ B- $\alpha$  ubiquitination and degradation. *Cell Microbiol.* 2008;10(9):1879–92.
107. Misaghi S, et al. *Chlamydia trachomatis*-derived deubiquinating enzymes in mammalian cells during infection. *Mol Microbiol.* 2006;61(1):142–50.
108. Li Z, et al. Induction of protective immunity against *Chlamydia muridarum* intravaginal infection with a chlamydial glycogen phosphorylase. *PLoS One.* 2012;7(3):e32997.
109. Lu C, et al. *Chlamydia trachomatis* GlgA is secreted into host cell cytoplasm. *PLoS One.* 2013;8(7):e68764.
110. Swanson KA, et al. *Chlamydia trachomatis* polymorphic membrane protein D is an oligomeric autotransporter with a higher-order structure. *Infect Immun.* 2009;77:508–16.
111. Werhl W, et al. From the inside out — processing of the chlamydial autotransporter Pmp D and its role in bacterial adhesion and activation of human host cells. *Mol Microbiol.* 2004;51(2):319–34.
112. Nunes A, Gomes JP, Karunakaran KP, Brunham RC. Bioinformatic analysis of *Chlamydia trachomatis* PmpE, PmpF, PmpG and PmpH as potential vaccine antigens. *PLoS One.* 2015;10(7):e0131695.
113. Tan C, Spitznagel JK, Shou HZ, et al. The polymorphic membrane protein gene family of the chlamydiae. In: Bavoil PM, Wyrick PB, editors. *Chlamydia: genomics and pathogenesis*. Norfolk: Horizon Bioscience; 2006. p. 195–218.
114. Liu X, et al. Identification of *Chlamydia trachomatis* outer membrane complex proteins by differential proteomics. *J Bacteriol.* 2010;192(11):2852–60.

Submit your next manuscript to BioMed Central and we will help you at every step:

- We accept pre-submission inquiries
- Our selector tool helps you to find the most relevant journal
- We provide round the clock customer support
- Convenient online submission
- Thorough peer review
- Inclusion in PubMed and all major indexing services
- Maximum visibility for your research

Submit your manuscript at  
[www.biomedcentral.com/submit](http://www.biomedcentral.com/submit)

